ENVIRONMENTAL RESEARCH
FOOD SYSTEMS

PURPOSE-LED PUBLISHING™

Part of the ENVIRONMENTAL RESEARCH SERIES

PAPER • **OPEN ACCESS**

Projected spatiotemporal changes in U.S. crop conditions under future climate scenarios

To cite this article: Logan R Bundy *et al* 2026 *Environ. Res.: Food Syst.* **3** 035016

View the article online for updates and enhancements.

You may also like

- Stochastically modeling the projected impacts of climate change on rainfed and irrigated US crop yields
  Xiao Zhu, Tara J Troy and Naresh Devineni
- Uncertainty in future agro-climate projections in the United States and benefits of greenhouse gas mitigation
  Erwan Monier, Liyi Xu and Richard Snyder
- Why are agricultural impacts of climate change so uncertain? The importance of temperature relative to precipitation
  David B Lobell and Marshall B Burke

This content was downloaded from IP address 24.14.116.219 on 27/07/2026 at 03:04

IOP Publishing Environ. Res.: Food Syst. 3 (2026) 035016 https://doi.org/10.1088/2976-601X/ae885b

ENVIRONMENTAL RESEARCH
FOOD SYSTEMS

Check for updates

OPEN ACCESS

RECEIVED
20 April 2026

REVISED
1 July 2026

ACCEPTED FOR PUBLICATION
9 July 2026

PUBLISHED
21 July 2026

Original content from this work may be used under the terms of the Creative Commons Attribution 4.0 licence.

Any further distribution of this work must maintain attribution to the author(s) and the title of the work, journal citation and DOI.

PAPER

Projected spatiotemporal changes in U.S. crop conditions under future climate scenarios

Logan R Bundy[1,*], **Vittorio A Gensini**[1], **Walker S Ashley**[1], **Alex M Haberlie**[1], **Allison C Michaelis**[2] and **David Changnon**[1]

[1] Department of Earth, Atmosphere and Environment, Northern Illinois University, DeKalb, IL, United States of America
[2] Department of Marine, Earth, and Atmospheric Sciences, North Carolina State University, Raleigh, NC, United States of America
[*] Author to whom any correspondence should be addressed.

E-mail: lbundy@niu.edu

Keywords: crop conditions, climate, agroclimatology, yield

Supplementary material for this article is available online

Abstract

This study integrates historical crop condition ratings with high-resolution regional climate simulations to quantify how U.S. crop conditions may evolve under intermediate and pessimistic anthropogenic emissions scenarios. State-, month-, and crop-specific gradient-boosted tree models were trained using climate predictors related to temperature, precipitation, water balance, and soil moisture. These models were used to compare late-twentieth-century crop conditions (1990–2005) with projected mid-century (2040–2055) and late-century (2085–2100) conditions. Because non-climate factors such as technology, management, genetics, and adaptation are held constant for modeling purposes, the results represent a baseline estimate of climate-driven crop condition risk. Projections indicate widespread declines in crop condition ratings, with declines generally intensifying and becoming more spatially coherent from mid- to late-century under higher emissions. The most robust declines occur from July onward, coinciding with reproductive crop development and yield formation. These changes are consistent with projected warming, reduced mean precipitation totals, and greater precipitation variability across key agricultural regions. Nationally, crop conditions are also projected to become more variable from year to year for most crops. Variability increases are largest during the late-vegetative to reproductive transition, thereby increasing uncertainty during the most yield-sensitive period of the summer growing season. Regionally, production risk depends on both changes in mean conditions and changes in variability. Northern U.S. small grains and portions of Midwest row crops are projected to experience declining mean conditions and increasing interannual variability, while many southern U.S. cropping systems exhibit more persistent condition declines. These findings provide a climate-driven basis for agricultural policy and adaptation planning by identifying where crop monitoring, risk management programs, water resource planning, and regional resilience strategies may be most needed to sustain agricultural production through the twenty-first century.

1. Introduction

The resilience and stability of U.S. crop production have far-reaching implications for both domestic prosperity and the global food supply chain. Not only does the agricultural system face mounting pressure from rising global population (Jung *et al* 2021), but recent trends and future climate projections suggest these pressures will be exacerbated by increasing temperatures (Dittus *et al* 2015, Vose *et al* 2017, Angel *et al* 2018), shifting precipitation regimes in the form of increasing drought occurrences (Jin *et al* 2017, Wehner *et al* 2017, Martin *et al* 2020), extreme precipitation events (Easterling *et al* 2017, Changnon and Gensini 2019, Stinnett *et al* 2024), and favorable severe thunderstorm environments across key U.S. agricultural regions (Brimelow *et al* 2017, Gensini and Brooks 2018, Tang *et al*

© 2026 The Author(s). Published by IOP Publishing Ltd

2019, Allen *et al* 2020, Gensini 2021, Ashley *et al* 2023, Gensini *et al* 2024, Haberlie *et al* 2024, Kaminski *et al* 2025).

Not only do weather- and climate-related hazards affect agriculture through direct yield losses, but they also alter the environmental and biological conditions that govern crop development throughout the growing season. As a result, the accelerating rate of these changes may impose increased biotic pressures on crops (Hurburgh 2016, Jinger *et al* 2017, Ramesh *et al* 2017, Wienhold *et al* 2018, Angel *et al* 2018), change phenological stage timing (Delgado *et al* 2013), and degrade soil integrity (Cai *et al* 2015, Hatfield *et al* 2015). Consequently, escalating risks to crop quality and yield demand robust, quantitative assessment to determine how agricultural systems may evolve under future climate scenarios.

During the latter half of the twentieth century, observed yield gains for major U.S. crops were largely driven by advances in management, genetics, and technology, resulting in nearly a two-fold increase in crop yields since the 1970s (Petersen 2019, USDA 2025a). However, recent observations and twenty-first-century projections reveal crop- and region-specific yield responses, underscoring the influence of climate variability and weather extremes (Rosenzweig *et al* 2014, Kukal and Irmak 2018, Jagermeyr *et al* 2021, Rezaei *et al* 2023). Both statistical and process-based modeling indicate that future yield trends will be shaped by temperature extremes and precipitation variability, with these factors projected to reduce yields for major staple crops across the U.S. (e.g. Lobell and Asseng 2017, Roberts *et al* 2017, Schauberger *et al* 2017, Zhu *et al* 2019, Bolster *et al* 2023, Fei *et al* 2023, Proctor *et al* 2025). When technological change is considered, projections indicate that stagnant innovation exacerbates climate-driven yield declines, whereas sustained advances in genetics and management can help mitigate or partially offset negative yield returns (Huffman *et al* 2018, Petersen 2019, Burchfield *et al* 2020, Hultgren *et al* 2025). Nevertheless, most yield-projection frameworks focus on end-of-season yield outcomes, providing limited insight into the in-season evolution of crop conditions and cumulative stress exposure that ultimately determine harvest outcomes. As a result, crop condition metrics that directly reflect these in-season dynamics remain underused in agroclimatic assessments.

Weekly assessments of crop conditions are essential for estimating crop yield outcomes and for enabling timely, data-informed decisions across a broad range of stakeholders (Lehecka 2014, Khaki *et al* 2021). One of the most widely used tools for monitoring crop quality in the U.S. is the USDA National Agricultural Statistics Service (NASS) crop progress and condition report (CPCR). These weekly, subjective condition reports are routinely used to forecast crop yields at the state and national level (Irwin and Good 2017a, 2017b, Irwin and Hubbs 2018a, 2018b, Beguería and Maneta 2020, Bundy and Gensini 2022, Bundy *et al* 2024, 2025a), quantify impacts on agricultural futures markets (Bain & Fortenbery 2017, Lehecka 2014, Karali *et al* 2016, Fernandez-Perez *et al* 2019, McKenzie and Ke 2022), and evaluate crop condition responses to extreme weather perils (Bundy *et al* 2023, 2026a). Although several objective approaches exist for monitoring crops during the growing season (e.g. satellite products), subjective crop condition assessments that rely on human observers integrate agronomic expertise and local context, capturing aspects of crop conditions that are often difficult to resolve using remote sensing alone (Beguería and Maneta 2020, Bundy *et al* 2026b). Long-term condition trends further underscore the importance of sustained monitoring, as crop condition ratings have declined since the mid-1980s across major U.S. agricultural regions (Bundy *et al* 2024, 2025a). While national yield trends have not yet mirrored these condition declines, persistent degradation in crop conditions may constrain future yield growth should the pace of these advancements slow or if adverse climatic trends continue.

Despite widespread use of USDA crop condition ratings for real-time monitoring, their application to future climate-impact assessment remains largely unexplored. Most agricultural climate-impact studies focus on end-of-season yield outcomes, leaving limited understanding of how crop stress may evolve during the growing season before harvest. This study addresses that gap by developing a novel framework for projecting future USDA crop condition ratings across the mid- and late-twenty-first century at the state and national level. To our knowledge, this is among the first studies to integrate USDA crop condition indices with high-resolution, dynamically downscaled regional climate simulations to project future in-season crop conditions. Weekly crop condition ratings are modeled for nine major U.S. crops: barley (*Hordeum vulgare* L.), corn (*Zea mays* L.), cotton (*Gossypium hirsutum* L.), oats (*Avena sativa* L.), peanuts (*Arachis hypogaea* L.), sorghum (*Sorghum bicolor* L.), soybeans (*Glycine max* L.), and spring and winter wheat (*Triticum aestivum* L.).

By integrating crop condition indices with climate variables, this framework captures both the temporal evolution and spatial variability of crop health in a way that complements traditional yield-projection approaches. Rather than focusing only on final harvest outcomes, this approach provides insight into when and where climate-driven stress may emerge during the growing season. Ultimately, modeling the potential future of U.S. crop conditions provides a bridge between agronomic understanding and actionable foresight, supporting more resilient agricultural systems in an era of accelerating change.

2. Methods

2.1. USDA crop condition data

The USDA invests resources to collect, process, and disseminate data through its weekly CPCR, relying on extension agents and farm service agency staff with extensive agronomic expertise. Data for the CPCR are collected through an extensive national reporting network comprising approximately 3600 respondents, with at least one or two reporters per county, collectively representing more than 75% of total U.S. crop production (USDA 2025b). Respondents are asked to provide subjective assessments of crop progress and condition based on standardized USDA definitions for the week ending on Sunday (USDA 2025b). For crop conditions, respondents estimate the percentage of each evaluated crop falling into five condition categories: excellent, good, fair, poor, and very poor. These categories are defined using consistent national criteria to ensure comparability across crops, regions, and growing seasons (USDA 2016):

- *Excellent*: yield prospects are above normal. Crops are experiencing little or no stress. Disease, insect damage, and weed pressure are insignificant.
- *Good*: yield prospects are normal. Moisture levels are adequate, and disease, insect damage, and weed pressures are minor.
- *Fair*: less-than-normal crop condition. Yield loss is a possibility, but the extent is unknown.
- *Poor*: heavy degree of loss to yield potential, which can be caused by excess soil moisture, drought, disease, etc.
- *Very Poor*: extreme degree of loss to yield potential; complete or near crop failure.

The USDA-defined crop condition index (CCIndex) was calculated for each report using the following (Rosales 2021):

$$\text{CCIndex} = \frac{1}{100}\left(5P_{\text{excellent}} + 4P_{\text{good}} + 3P_{\text{fair}} + 2P_{\text{poor}} + P_{\text{very poor}}\right)$$

where $\mathrm{P}_{\text{excellent}}$, P_{good}, P_{fair}, P_{poor}, and $\mathrm{P}_{\text{very poor}}$ represent the percentage of the crop rated in each USDA condition category. The CCIndex aggregates weekly crop condition reports across the five USDA condition categories into a single metric. Values range from 1 to 5, where a value of 5 corresponds to 100% of the crop rated in excellent condition and a value of 1 indicates that 100% of the crop is rated as very poor. Because excellent and good condition ratings are generally associated with normal to above-normal yield potential, increases in these categories result in higher CCIndex values (supplemental figure 1). Conversely, fair, poor, and very poor ratings have a negative effect on the CCIndex (Bundy *et al* 2024). The CCIndex was used as the primary modeling variable because it incorporates the full distribution of condition categories, thereby retaining more information about the overall spectrum than aggregated metrics such as good + excellent (Bain and Fortenbery 2017). By incorporating all five USDA condition categories, the CCIndex provides a continuous measure of overall crop condition that captures shifts across the full rating distribution, including changes that may be missed when evaluating a single category alone. However, because the CCIndex is less intuitive, good-to-excellent ratings were used as a supplementary benchmark to translate changes in the CCIndex into operationally meaningful context. Specifically, a ±0.1 change in the CCIndex corresponds to a ±4%–6% change in good-to-excellent ratings across all crops used in this study (supplemental figure 1).

To ensure reliability, NASS applies multiple quality control procedures to each reported observation, which include evaluating consistency and plausibility through comparisons with prior weekly reports, long-term averages, and reports from neighboring counties (USDA 2025b). Following this review, USDA field offices aggregate county-level data to the state level, with individual reports weighted by NASS acreage estimates to reflect the spatial distribution of crop production (USDA 2025b). State-level summaries are then submitted to the Agricultural Statistics Board, where they undergo additional evaluation in the context of surrounding states before being aggregated to national estimates (USDA 2025b). National-level crop condition values are computed using a weighting scheme based on each state's three-year mean planted acreage for the respective crop (USDA 2025b).

State-level crop condition data were collected from the USDA NASS QuickStats database for the nine crops analyzed (USDA 2025a). Weekly condition records were used from 1986 to 2024 for all crops except barley, oats, and peanuts, for which complete records spanned from 1996 to 2024. For sufficient data continuity, states and weeks were included only if at least 90% of weekly observations were available over the study period, following the same criteria outlined in Bundy *et al* (2024). Missing weekly observations were not interpolated. Instead, state-crop-week combinations that did not meet the 90% availability threshold were excluded from the analysis. Most missing observations occurred near the beginning or the end of the crop reporting season, when USDA condition reporting is often less consistent across states and crops due to varied planting and harvest times from year to year.

2.2. WRF-BCC climate simulations

Projections from dynamically downscaled regional climate simulations were obtained from the Weather Research and Forecasting-Bias Corrected Community Earth System Model (WRF-BCC CESM), a convection-permitting regional climate modeling framework developed for the conterminous U.S. (Gensini *et al* 2023). Dynamical downscaling (e.g. Prein *et al* 2015) enables both implicit and explicit representation of hazardous convective weather at a high resolution (Gensini *et al* 2023). WRF-BCC data consist of three 15-year simulation epochs representing historical climate environments (HIST; 1990–2005), mid-century projections (MID; 2040–2055), and end-of-century projections (END; 2085–2100). WRF-BCC simulations were developed using the Advanced Research core of the WRF model (WRF-ARW v.4.1.2), which is a fully compressible nonhydrostatic model widely used in operational weather forecasting and research (Skamarock and Klemp 2008, Skamarock *et al* 2019, Gensini *et al* 2023). Initial and lateral boundary conditions were forced by a bias-corrected version (Bruyere *et al* 2014) of the CESM global climate model output (CESM; Hurrell *et al* 2013), a participant in phase 5 of the Coupled Model Intercomparison Project (CMIP5; Taylor *et al* 2012). WRF-BCC has a horizontal grid spacing of 3.75 km, providing high-resolution simulations capable of representing localized precipitation and convective weather processes more directly than coarser climate models (Weisman *et al* 1997, Skamarock and Klemp 2008, Westra *et al* 2014).

Each WRF-BCC simulation was continuously integrated over individual hydrologic years (1 October–30 September), with reinitialization occurring annually on 1 October (Gensini *et al* 2023). Future period simulations were conducted under representative concentration pathways (RCPs) 4.5 and 8.5 (Moss *et al* 2010), as used in the Intergovernmental Panel on Climate Change fifth assessment report (IPCC 2014). RCP 4.5 represents an intermediate future climate in which radiative forcing and greenhouse gas concentrations stabilize by 2100 without overshoot, whereas RCP 8.5 represents a high-emissions pathway characterized by substantially greater radiative forcing that is nearly double that of RCP 4.5 (Moss *et al* 2010). Although RCP 8.5 is considered a high-emissions or high-forcing scenario rather than the most likely future pathway, it remains widely used in climate impact research as a benchmark for evaluating upper-bound climate responses and associated risks (Hausfather and Peters 2020, Schwalm *et al* 2020). While a less probable future, the continued use of RCP 8.5 facilitates comparisons with the extensive body of literature based on CMIP5 projections and provides insight into the potential magnitude of climate impacts under stronger radiative forcing, but should be interpreted with caution. Further details on the WRF-BCC model configuration and its verification are provided in Gensini *et al* (2023).

Although newer climate projections increasingly use the shared socioeconomic pathway (SSP) framework in CMIP6, the RCP framework remains widely used in regional climate impact studies. Because WRF-BCC simulations employed here were developed using forcing data consistent with the CMIP5 generation of models (Gensini *et al* 2023), the use of RCP 4.5 and RCP 8.5 provides consistency with the underlying climate model configuration. Moreover, comparisons between CMIP5 RCP scenarios and their CMIP6 SSP counterparts indicate that projected climate responses at comparable radiative forcing (e.g. RCP 4.5 versus SSP2-4.5 and RCP 8.5 versus SSP5-8.5) are broadly similar in terms of temperature and precipitation trends, particularly during the mid-century (Tebaldi *et al* 2021). Thus, the continued use of RCP scenarios remains relevant for studies using CMIP5-based regional climate simulations and facilitates direct comparison with the large body of existing climate impact literature.

Daily precipitation totals at each 3.75 km grid cell were derived from the Air Force Weather Agency (Creighton *et al* 2014) accumulated precipitation variable, archived at 15 min temporal resolution, and aggregated to daily values. The precipitation variable is the accumulation of all precipitation from convection and microphysics schemes. In addition, daily minimum and maximum 2 m air temperature fields were extracted from WRF-BCC output but were unavailable for RCP 4.5 during the END period. Therefore, modeling efforts for that period were omitted in this study. WRF-BCC simulations were originally designed and archived for research focused on mesoscale convective systems and related high-impact weather, and not all variables were retained for every scenario and epoch because of the large data volumes produced by convection-permitting climate simulations. End-of-century RCP 4.5 was excluded rather than applying a different model structure or introducing non-comparable predictors. End-of-century projections were therefore limited to RCP 8.5. The four simulation periods used in this analysis, each spanning 15 hydrologic years, are hereafter referred to as HIST, MID45, MID85, and END85. Each of the three variables was aggregated to the county level by computing the mean of all grid cells intersecting each county. High spatial (3.75 km) and temporal (15 min) resolution of WRF-BCC simulations is particularly important for this study because of its ability to simulate deep convection, mesoscale convective systems, and localized heavy precipitation, and these occur at spatial scales that are generally not resolved in traditional coarse global climate models (Prein *et al* 2015, Kendon *et al* 2017). Therefore, this resolution enables aggregation to counties using numerous grid cells per unit area, preserving meaningful spatial heterogeneity and enhancing the ability to assess agroclimatic stress at the field level. While WRF-BCC represents only a single future climate outcome, previous applications of the regional climate model simulation have proven effective for examining future changes in high-impact weather extremes (e.g. Ashley *et al* 2023, Gensini *et al* 2024, Haberlie *et al* 2024, Stinnett *et al* 2024, Zeeb *et al* 2024, Kaminski *et al* 2025, Wallace *et al* 2025) and provide a credible framework for agroclimatic risk assessment.

2.3. Parameter-elevation regressions on independent slopes model (PRISM) climatological data

Daily precipitation, minimum temperature, and maximum temperature data were obtained from the Parameter-elevation Regressions on Independent Slopes Model (PRISM; Daly *et al* 1994) for the 1986–2024 period (PRISM 2025). PRISM is an observationally based, high-resolution climate dataset provided on an approximately 4 km grid, incorporating interpolation and bias-adjustment techniques that leverage multiple quality-controlled observational inputs. While PRISM does not represent direct ground truth, its major strengths lie in its consistent spatiotemporal coverage, fine spatial resolution, and extensive quality control, making it well suited for agroclimate applications. Previous evaluations demonstrate strong agreement between PRISM and WRF-BCC, with Pearson correlation coefficients of 0.99 for historical annual mean 2 m air temperature and 0.91 for annual mean precipitation, despite the presence of some regional and seasonal biases (Gensini *et al* 2023). Daily PRISM fields were spatially aggregated to the county level by computing the mean value of all grid cells intersecting each county boundary, consistent with the WRF-BCC data aggregation to the county level.

2.4. Model variables

Daily, county-level maximum and minimum temperature and precipitation from PRISM were used to construct a comprehensive suite of agronomically relevant predictor variables designed to capture both short-term weather extremes and antecedent hydroclimatic conditions for the 1986–2024 period. From these inputs, the following variables were derived: 7 d mean of maximum, minimum, and mean temperature; 7 d absolute maximum and minimum temperature; 7 d mean diurnal temperature range; weekly maximum 1 d precipitation; cumulative precipitation over 7-, 14-, 30-, and 60 d periods; and a series of hydrological metrics, including 7-, 14-, and 30 d water balance terms, and a soil moisture leaky bucket model (table 1). Together, these variables characterize thermal stress, moisture availability, and lag effects that are known to influence crop development and conditions across all phenological stages.

To calculate hydrological variables, potential evapotranspiration (PET) was estimated using the Hargreaves method, which approximates atmospheric evaporative demand from temperature and extraterrestrial radiation (Hargreaves and Samani 1982, Hargreaves and Allen 2003). Although the Penman–Monteith method is generally preferred when the necessary meteorological inputs are available (e.g. humidity, wind speed, net radiation), this study required a PET formulation that could be applied consistently across both the historical PRISM dataset and WRF-BCC climate simulations. The Hargreaves method was therefore selected because it relies on temperature variables that were available across all historical and future datasets, while solar radiation can be calculated consistently from latitude and day of year. This approach is computationally efficient, physically grounded, and well suited for large-scale, multi-decadal, and multi-scenario applications where radiation observations are limited. Daily PET was calculated as

$$PET = 0.0023 * (T\ mean + 17.8) * \sqrt{T\ max - T\ min} * R_a$$

where R_{a} is daily incoming solar radiation at the top of the atmosphere, expressed in water-equivalent units (mm d^{-1}), and Tmean, Tmax, and Tmin represent the mean, maximum, and minimum daily temperature, respectively. R_{a} was computed following Hargreaves' formulations as a function of latitude and day of year, with latitude obtained from the centroid of each county. Radiation estimates were

Table 1. Climatic predictor variables used in the CCIndex modeling framework.

Variable	Abbreviation	Temporal aggregation	Units	Agroclimatic interpretation
7 d cumulative precipitation	P_{7d}	Cumulative total over prior 7 d	mm	Short-term moisture input during the reporting week
14 d cumulative precipitation	P_{14d}	Cumulative total over prior 14 d	mm	Antecedent wetness or dryness over the previous two weeks
30 d cumulative precipitation	P_{30d}	Cumulative total over prior 30 d	mm	Monthly-scale moisture availability and persistence
60 d cumulative precipitation	P_{60d}	Cumulative total over prior 60 d	mm	Longer-term antecedent precipitation and drought/wetness memory
Maximum 1 d precipitation	P_{max}	Maximum daily precipitation total within the reporting week	mm	Short-duration heavy precipitation and excess-moisture potential
Mean maximum temperature	$T\text{max}_{7d}$	Mean daily maximum temperature over prior 7 d	°C	Daytime heat exposure and thermal stress
Mean minimum temperature	$T\text{min}_{7d}$	Mean daily minimum temperature over prior 7 d	°C	Nighttime warmth and reduced overnight recovery
Mean air temperature	$T\text{mean}_{7d}$	Mean daily temperature over prior 7 d	°C	Overall weekly thermal environment
Absolute maximum temperature	$T\text{max}_{abs}$	Highest daily maximum temperature within the reporting week	°C	Acute heat exposure and extreme-temperature stress
Absolute minimum temperature	$T\text{min}_{abs}$	Lowest daily minimum temperature within the reporting week	°C	Cold exposure or minimum-temperature stress
Diurnal temperature range	DTR_{7d}	Mean daily Tmax-Tmin over prior 7 d	°C	Day-night temperature variability and thermal amplitude
7 d water balance	WB_{7d}	7 d precipitation minus 7 d PET	mm	Short-term atmospheric moisture surplus or deficit
14 d water balance	WB_{14d}	14 d precipitation minus 14 d PET	mm	Two-week moisture surplus or deficit
30 d water balance	WB_{30d}	30 d precipitation minus 30 d PET	mm	Monthly-scale hydroclimatic stress
Leaky-bucket soil moisture storage	SM_t	Daily leaky-bucket storage updated from water balance; summarized to weekly reporting period	mm	Standardized antecedent moisture-storage index representing cumulative wetness or dryness

derived using Earth–Sun geometry, explicitly accounting for inverse relative Earth–Sun distance, solar declination, and sunset hour angle (Hargreaves and Samani 1982, Hargreaves 1994). Daily PET values were subsequently aggregated to weekly totals by summation, consistent with the temporal resolution of the crop condition data and other predictor variables. Because Hargreaves does not explicitly represent aerodynamic controls, humidity effects, or vapor-pressure deficit as fully as Penman–Monteith, PET and the resulting water-balance variables are to be interpreted as relative indicators of atmospheric moisture demand and hydroclimatic stress rather than exact estimates of crop evapotranspiration.

To characterize short-term atmospheric moisture stress, a climatic water balance metric was computed and defined as the difference between precipitation and PET (Thornthwaite 1948, Thornthwaite and Mather 1955):

$$\mathrm{WB}_t = P_t - \mathrm{PET}_t$$

where P represents cumulative precipitation over the 7-, 14-, or 30 d period, and PET represents cumulative potential evapotranspiration over the same period. Including water balance at multiple temporal scales enables the modeling framework to distinguish between rapidly developing moisture deficits or surpluses and more persistent hydroclimatic anomalies that influence crop conditions over extended periods. To further represent cumulative plant-available soil moisture and wetness conditions, a simple leaky-bucket soil moisture model was implemented (Thornthwaite and Mather 1957, Manabe 1969, Westenbroek *et al* 2018):

$$\mathrm{SM}_t = \min\left(C,\ \max\left(0,\ \mathrm{SM}_{t-1} + \mathrm{WB}_t\right)\right)$$

where SM_t denotes soil moisture storage (mm) on day t, C is the soil water holding capacity, and WB_t is the daily climatic water balance. Soil water-holding capacity was uniformly set to 1000 mm across all counties, and storage was constrained between zero and the maximum capacity. This value was used as a simplified storage ceiling to represent cumulative antecedent wetness and dryness rather than a physically calibrated estimate of local plant-available soil water. A spatially uniform capacity was selected to maintain consistency with the climate-only design of the study and to avoid introducing soil, rooting-depth, irrigation, and management heterogeneity that cannot be directly separated from USDA CPCR. The resulting soil moisture variable should therefore be interpreted as a standardized antecedent moisture-storage index derived from precipitation and PET, not as a field-scale representation of actual soil water availability. As a robustness check, alternative bucket capacities were also tested, and the broad direction and spatial pattern of projected CCIndex changes were not sensitive to the specific storage-capacity value.

All weekly predictor variables were first derived at the county level using PRISM for the full historical crop condition period (1986–2024) and, using identical formulations and temporal aggregations, from the WRF-BCC simulations for the HIST, MID45, MID85, and END85 periods (END45 was unavailable due to a missing temperature variable). County-level variables were then aggregated to the state and national level following USDA NASS acreage-weighting procedures for each respective crop and growing season (USDA 2025b). For the future periods, a fixed 5-year (2020–2024) county acreage mean was used, isolating the influence of climate change on crop conditions while holding the spatial distribution of agricultural production constant.

The fifteen weekly predictors were selected to represent complementary dimensions of agroclimatic stress, including short-term precipitation, antecedent moisture availability, heat exposure, diurnal temperature variability, atmospheric water demand, and cumulative moisture storage. Further, the modeling framework was designed to estimate the climate-driven component of CCIndex variability using variables that could be constructed consistently across the historical PRISM data and future WRF-BCC simulations. Therefore, projections should be interpreted as conditional on the selected climate-variable set rather than as a complete representation of all factors influencing crop condition ratings. Non-climate factors such as soil properties, irrigation, pest and disease pressure, cultivar selection, management practices, and technological change were not explicitly included as predictors.

2.5. Crop condition modeling

The CCIndex was modeled using extreme gradient boosting (XGBoost) regression (figure 1), a tree-based ensemble learning method that is trained by sequentially fitting decision trees to the residuals of prior trees (Chen and Guestrin 2016). XGBoost is well-suited for agroclimatological applications since it resolves nonlinear crop–climate responses, threshold behavior, and interactions among climate variables without requiring explicit functional assumptions (Mariadass *et al* 2022). A common set of XGBoost parameters was used for all state-, crop-, and month-specific models to ensure a consistent modeling framework across regions and commodities. Parameter configuration was selected to favor conservative, regularized models suitable for relatively small samples for machine learning. Model settings included 1200 trees with a low learning rate of 0.03, allowing gradual boosting while limiting abrupt model updates. A maximum tree depth of 3 was used to capture nonlinear responses and low-order interactions without allowing overly complex trees. Subsample and column-sampling fractions of 0.7, a minimum child weight of 10, and L2 and L1 regularization terms of 2.0 and 0.1, respectively, were used to reduce overfitting and improve generalization across withheld years. Gamma was set to 0, and additional overfitting control was provided through regularization, subsampling, and early stopping. Models were implemented using the histogram tree-construction algorithm with a fixed random seed of 42 to ensure reproducibility.

The method is robust to multicollinearity, accommodates mixed predictor scales, and performs well with moderately sized datasets typical of state-level agricultural observations (Mariadass *et al* 2022). Separate models were trained for each state, crop, and month combination, allowing relationships between climate drivers and crop conditions to vary by geography, commodity, and phenological stage. Fifteen predictor variables (table 1) were derived from daily precipitation, minimum temperature, and maximum temperature fields using consistent formulations for the historical PRISM data and WRF-BCC climate simulations. The response variable (CCIndex) was bounded between 1 and 5, and treated as a continuous, inclusive variable, reflecting the underlying proportion-based construction of crop condition ratings rather than discrete classes. The training data were taken from the 1986 to 2024 period for all crops except barley, oats, and peanuts, for which the period was 1996–2024. A regression-based framework was retained to preserve subclass variability within the CCIndex and to enable smoother representation of climate–crop responses that may not be captured using strictly categorical approaches.

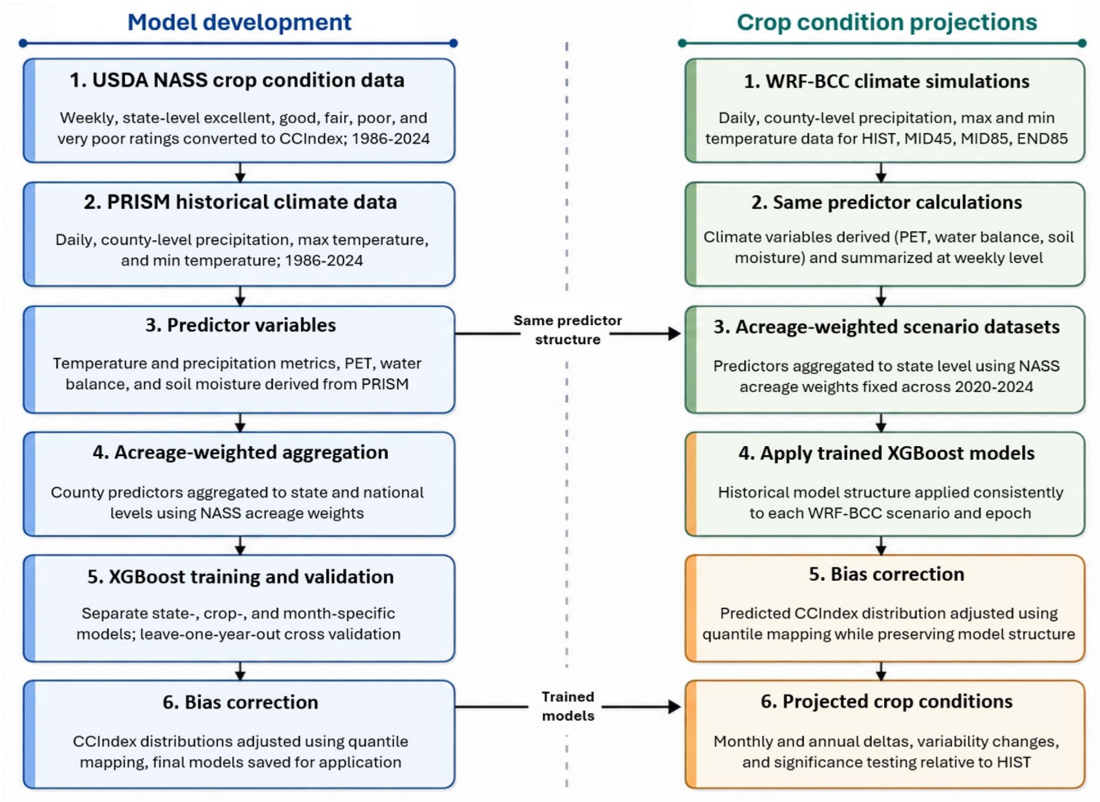

Figure 1. Workflow for developing historical CCIndex models and applying them to WRF-BCC climate scenarios to project future crop condition changes.

To assess out-of-sample performance, models were evaluated using a leave-one-year-out cross-validation framework to preserve temporal independence. This approach was selected because weekly crop condition observations within the same growing season are not independent; weather anomalies, management conditions, and crop responses can often persist across multiple weeks in a given year. Other validation procedures, such as random *k*-fold, could place observations from the same year in both the training and validation sets, potentially inflating model performance by allowing the model to learn year-specific conditions. Leave-one-year-out validation provides a more conservative assessment of generalizability by requiring the model to predict crop conditions for entirely withheld growing seasons. In each iteration, all observations from a single year were withheld for validation, and the model was trained on the remaining years, ensuring that validation is performed on temporally independent data and provides a more realistic assessment of model generalizability to unseen growing seasons. This rotating procedure ensured that every year served as validation data exactly once, yielding full out-of-sample predictions for all observations. With each training fold, early stopping was applied when sufficient data were available by using the most recent year from the training set as an internal evaluation year. Training was stopped if validation root mean squared error (RMSE) did not improve for 50 rounds, reducing potential overfitting while preserving the leave-one-year-out validation structure. Model performance was examined using both coefficient of determination (R^2) and RMSE, which reflect explained variance and absolute error between the modeled and observed CCIndex, respectively. After validation, a final XGBoost model was trained using all available data for each state-crop-month combination. These final models were saved and later applied to the WRF-BCC data using identical predictor structures.

Although the XGBoost models captured variability in crop condition ratings, tree-based boosting ensemble methods can still exhibit bias in the mean and spread of predictions, particularly across the tail ends of the distribution (supplemental figure 2). To correct these distributional biases while preserving model variability, a non-parametric quantile mapping approach was applied (Cannon *et al* 2015), which aligns the cumulative distribution function of the modeled CCIndex with that of the observed CCIndex by mapping each predicted value to its corresponding percentile in the observed distribution. Specifically, for each crop-state-month grouping, empirical cumulative distribution functions were constructed from the training data, and modeled values were transformed by matching their percentile in the modeled distribution to the equivalent percentile in the observed distribution. This approach corrects biases in the mean, variance, skewness, and extremes without altering the rank structure of the modeled values, thereby retaining the temporal variability learned by the model and ensuring consistency with the observed distribution of the CCIndex.

Differences in CCIndex distributions between the HIST and future WRF-BCC scenarios were evaluated using two-sample Welch's *t*-tests (Welch 1947) to assess whether the scenario-mean CCIndex ratings differed significantly from HIST at the 0.05 significance level. For each crop-state combination, CCIndex values were summarized to monthly and annual means, and scenario deltas were computed as the difference in mean CCIndex relative to HIST. In addition to mean changes, interannual variability was quantified as the standard deviation of monthly or annual mean CCIndex within each epoch, and differences in variability between HIST and each future scenario were tested for statistical significance at the 0.05 significance level using the Brown–Forsythe test (Brown and Forsythe 1974). The same set of hypothesis tests was applied to monthly regional mean temperature and precipitation from WRF-BCC to contextualize projected CCIndex changes in terms of underlying climate shifts. WRF-BCC variables (precipitation and mean temperatures) were aggregated by USDA Farm Production region, consisting of the Northwest, Southwest, Northern Plains, Southern Plains, Midwest (a combination of the Corn Belt and Lake region), Delta, Southeast, and Northeast (Cooter *et al* 2012).

2.6. Model verification and interpretation

When bias-corrected CCIndex values were aggregated to the national and annual scale (and compared against observed CCIndex values for each crop), the modeled CCIndex explained at least 25% of the interannual variance in observed CCIndex ratings and yielded RMSE values ranging from 0.08 to 0.15 for all crops (figure 2 and supplemental figure 3). Given the relatively narrow range of annual national CCIndex variability, the RMSE range indicates that the bias-corrected model generally reproduced observed CCIndex ratings with small absolute errors. However, the lower R^2 values for some crops indicate only modest explanatory power, suggesting that climate predictors alone do not capture all sources of interannual crop condition variability. This limitation is expected because USDA crop condition ratings are also influenced by non-climate factors, including management practices, irrigation, pests, disease, and reporting uncertainty. Model performance was highest for sorghum, peanuts, soybeans, and spring wheat, where the explanatory power exceeded 60%, indicating stronger climate sensitivity or a closer alignment between the selected predictors and observed crop condition variability for these crops. The same model structure, predictor set, and bias-correction framework were then applied consistently across the HIST, MID45, MID85, and END85 climate simulations. No statistically significant differences were noted among monthly and annual HIST CCIndex, modeled CCIndex, and observed CCIndex ratings over the 1990–2005 period for all crops. Collectively, these results indicate that weather and climate conditions account for a substantial fraction of observed crop condition variance, while the remaining unexplained variance likely reflects survey-related noise, heterogeneity in agricultural management, and non-meteorological stressors that are not explicitly represented in the modeling framework.

Model interpretability was evaluated using aggregated feature importance and partial dependence analysis to identify the climatic drivers learned by the XGBoost framework and to assess whether the modeled responses were consistent with agronomic understanding. When feature importance was aggregated across all states, crops, and months, antecedent moisture availability emerged as the dominant control on predicted weekly CCIndex. The highest-ranked predictors were 60 d total precipitation, soil moisture, 30 d water balance, and 30 d total precipitation, all of which describe cumulative moisture supply rather than isolated daily weather conditions (supplemental figure 4). Therefore, this indicates that the model placed the greatest weight on the persistence of wet or dry conditions leading into the crop-condition observation period. Temperature-related variables, including weekly absolute maximum temperature, weekly mean diurnal temperature range, and weekly mean daily maximum temperature, also contributed to CCIndex prediction, but their relative importance was lower than that of the leading moisture-related predictors. Generally, this ranking is consistent with agronomic expectations and prior research showing that crop condition and yield are strongly influenced by the combined effects of precipitation, soil-water availability, and atmospheric demand, with heat stress often becoming most damaging when it occurs alongside moisture limitation (Li *et al* 2019, Bundy *et al* 2026b).

Learned relationships between climatic variables and CCIndex were also nonlinear and consistent with known crop-stress mechanisms (supplemental figure 5). Temperature predictors generally produced limited changes in predicted CCIndex across moderate values, followed by declines under higher thermal stress. For example, weekly absolute maximum temperature induced a negative response once values exceeded approximately 32 °C, which is consistent with empirical evidence that high temperatures can impair crop growth, reproductive development, and overall plant performance (Hatfield and Prueger 2015). Overall, this pattern suggests that short-term exposure to adverse temperatures can reduce crop

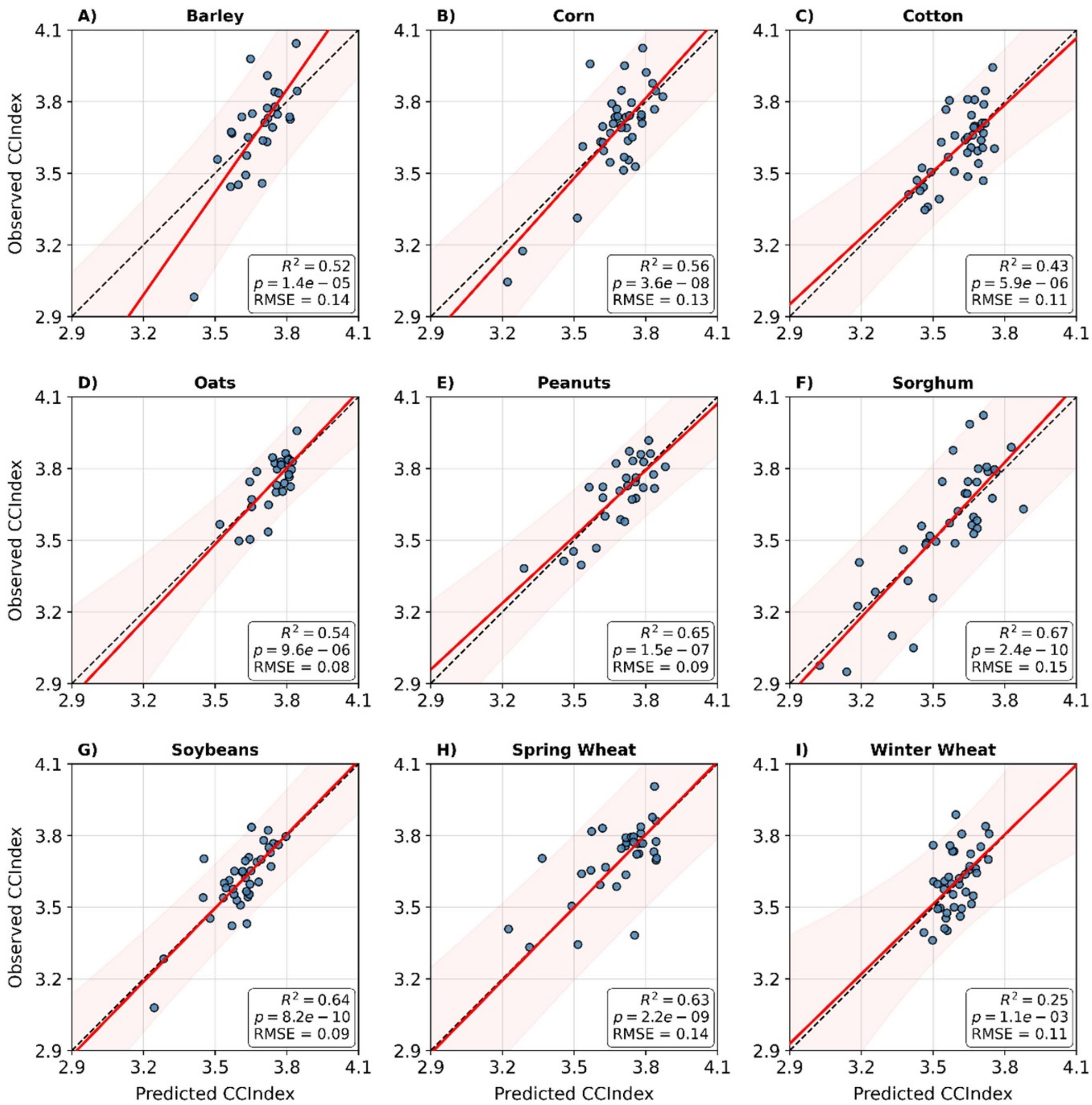

Figure 2. Observed USDA and predicted PRISM-derived CCIndex ratings for 1986–2024 by crop. The black dashed line indicates the 1:1 relationship, the red line shows the least-squares regression, and red shading represents the 95% prediction interval. Model statistics are reported in each panel.

condition, particularly when heat occurs during sensitive phenological periods. Moisture-related predictors produced the strongest partial dependence responses. In general, low antecedent precipitation, low soil moisture, and negative water balance were associated with lower predicted CCIndex values, while more favorable moisture conditions moved the response toward neutral or slightly positive values, whereas excessive moisture was associated with declines. For 60 d precipitation, the aggregated response displayed lower CCIndex values under relatively dry conditions below approximately 180 mm, while values above roughly 260 mm also corresponded to a modest decline, suggesting that both moisture deficits and excessively wet conditions may reduce crop condition. These thresholds should be interpreted as broad, aggregated patterns because the specific response values vary by crop, state, and phenological stage; however, the general relationships are consistent with previous work linking crop condition and yield variability to moisture stress, water-balance deficits, and heat exposure (Li *et al* 2019, Bundy *et al* 2026b).

Capturing nonlinear climate–crop relationships is a key component of crop-condition and yield modeling because crop responses to weather stress are rarely uniform across the full range of environmental conditions. Crops may tolerate moderate departures from optimal temperature or moisture conditions, but crop condition can deteriorate rapidly once soil-water deficits, heat stress, or atmospheric demand exceed physiological tolerance thresholds. The partial dependence results demonstrate that the XGBoost framework captured these threshold-like stress responses, particularly for low antecedent precipitation, low soil moisture, negative water balance, and elevated temperatures (supplemental figure 5).

This helps explain why the model was able to produce skillful CCIndex predictions—the strongest predictive signals were not only statistically important, but also aligned with known agronomic mechanisms. Therefore, the interpretability results increase confidence in the modeling framework by demonstrating that the XGBoost models learned physically meaningful relationships between climate variability and crop condition rather than relying solely on opaque statistical associations. Again, the modeling framework was intended to isolate the climate-driven component of CCIndex variability using predictors that could be consistently derived from both the historical PRISM dataset and the future WRF-BCC simulations. As a result, crop condition projections should be interpreted as responses to the selected climate-variable set, rather than as a complete representation of all climatic, management, biotic, and socioeconomic factors that can influence observed crop condition ratings.

3. Results

3.1. Seasonal progression of crop condition projections

Across nearly all crops and growing-season months, CCIndex ratings are projected to decline during both MID (2040–2055) and END (2085–2100) periods relative to HIST (1990–2005; figure 3). Although the magnitude of CCIndex rating changes varies by crop, monthly mean CCIndex responses generally align in terms of the direction of change across most crops examined. When averaged across all crops during MID (mean of MID45 and MID85), departures from HIST are modest early in the growing season (June and July) but progressively worsen later in the growing season, reaching −0.10 in August and September. Although differences in monthly mean CCIndex ratings from HIST are statistically significant for 55% of crop-month combinations during MID, these modest change magnitudes should be interpreted cautiously from an agronomic perspective. Scenario-specific patterns further highlight the strengthening signal in crop condition projections, as under MID45, 74% of crop-month combinations reveal CCIndex declines, whereas under MID85, the proportion of declining combinations increases to 100%. Agronomically, this seasonal pattern suggests that projected crop condition declines become more consequential later in the growing season, when many crops transition from vegetative growth into reproductive development and yield formation.

When examining individual crops during MID, sorghum, barley, spring wheat, and peanuts are projected to experience the largest CCIndex declines across both emission scenarios, with mean monthly deltas from HIST ranging from −0.02 to −0.28 (table 2), corresponding to good-to-excellent changes ranging from −1% to −17%. Nationally, only 26% of crop-month combinations contain conflicting trends between MID45 and MID85, increasing confidence in the projected crop condition trend between emission scenarios during the mid-century. As for the progression of CCIndex ratings through the growing season, projections suggest that each crop will undergo a worsening trend from emergence to harvest as the twenty-first century continues (table 3). As such, cotton, soybeans, sorghum, and peanuts experience the steepest in-season deterioration under MID45 and MID85, with mean CCIndex deltas ranging from −0.13 to −0.27 (good-to-excellent: −5% to −16%), representing a worsening trend relative to HIST changes of −0.10 to −0.22 (good-to-excellent: −4% to −13%). More moderate but still consistent negative seasonal deltas are present during MID for all other crops. Overall, projections during MID suggest not only a risk of lower mean intermonthly crop conditions but also an accelerating rate of degradation through the growing season for major U.S. crops. This late-season deterioration is especially relevant, as stress during reproductive and grain- or seed-filling stages can have a greater effect on final yield potential than comparable stress during earlier vegetative growth.

By END85, CCIndex declines are projected to become both more robust and consistent across the growing season, with mean CCIndex differences between END85 and HIST indicating statistical significance for 97% of all growing season crop-month combinations (figure 3 and table 2). When averaged across all crops, END85 mean CCIndex departures from HIST worsen as the season progresses, reaching −0.16 in June and progressively worsening through July and August before reaching −0.30 in September (good-to-excellent changes ranging −6% to −19% across the full summer growing season). The concentration of the strongest declines during July–September indicates that future climate stress is projected to intensify during the portion of the growing season when pollination, flowering, pod set, boll development, and grain or seed filling are most sensitive to heat and moisture stress. Among individual crops, sorghum, corn, soybeans, and peanuts undergo the most pronounced declines during END85, with mean CCIndex reductions relative to HIST ranging from −0.12 to −0.60, and the worst of these trend projections occurring during the latter portion of the growing season (July–September). Moreover, the END85 signal is directionally consistent with MID85, as none of the national crop-month combinations exhibit conflicting trend directions between the two scenarios. This alignment increases confidence

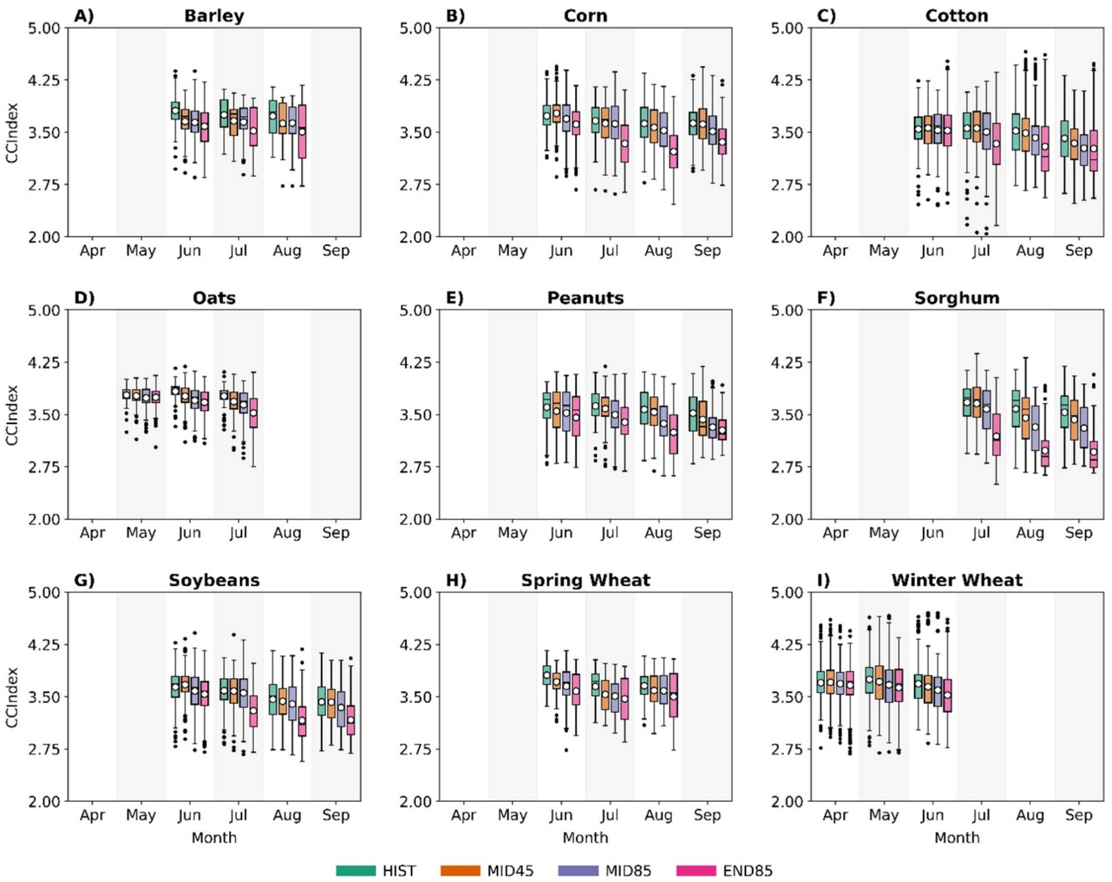

Figure 3. WRF-BCC-modeled monthly CCIndex ratings by scenario and crop. Points represent state-crop-month values; boxes show the interquartile range, black lines indicate medians, whiskers show 1.5× the interquartile range, and white squares indicate means.

in the sign of the projected CCIndex change, even though the magnitude of change remains scenario-dependent. Seasonal deterioration from emergence through harvest also intensifies under END85 across nearly all crops. The steepest mean CCIndex in-season changes during END85 are projected for soybeans (−0.36), followed by corn, cotton, oats, and all other crops, with slopes ranging from −0.08 to −0.25, corresponding to good-to-excellent rating changes ranging from −3% to −22%. When averaged across all crops, the mean in-season CCIndex delta from the first to last reporting week during HIST is −0.11, then −0.14 during MID45, −0.16 during MID85, and −0.20 during END85, indicating an accelerating rate of condition degradation as the growing season progresses.

Just as important as quantifying shifts in mean crop conditions is assessing how their distributions may change across scenarios, particularly changes in variability and frequency of extreme condition outcomes. Trends in CCIndex variability—defined here as the standard deviation of intermonthly mean CCIndex ratings for each epoch—are inversely related to trends in mean intermonthly CCIndex values across most crops. Nationally, oats, spring wheat, corn, and soybeans contain some of the strongest negative Pearson correlation coefficients between mean CCIndex deltas and standard deviation deltas ($R < -0.60$). Therefore, for most crops, monthly CCIndex standard deviations are projected to increase from HIST through END85 at an accelerating rate, underscoring not only poorer mean crop conditions but also a progressively more volatile growing season (figure 3; table 4). When averaged across all crops during MID (mean of MID45 and MID85), CCIndex variability increases subtly early in the growing season and peaks during mid-summer, with mean standard deviation departures from HIST of 0.01 in June and 0.02 in July, followed by departures −0.01 in August and September. Evidence of some consistency across emission scenarios further supports the robustness of variability signals, as 45% of crop-month combinations contain conflicting trends between standard deviation deltas during MID45 and MID85. In these mismatch cases, most of the variability transitions are from a decrease under MID45 to an increase under MID85. During MID85 specifically, 65% of crop-month combinations undergo CCIndex variability increases, with only one of those increases statistically significant, and the strongest and most consistent signals occurring in June and July. From an agronomic perspective,

Table 2. Monthly mean CCIndex deltas for each epoch (MID45, MID85, and END85) relative to HIST. Bold font indicates statistical significance at the 0.05 significance level.

Crop	Month	ΔMID45	ΔMID85	ΔEND85
Barley	June	**−0.15**	**−0.16**	**−0.22**
Barley	July	**−0.09**	**−0.11**	**−0.23**
Barley	August	−0.09	−0.09	**−0.22**
Corn	June	0.03	−0.04	**−0.14**
Corn	July	−0.04	−0.05	**−0.34**
Corn	August	**−0.06**	**−0.11**	**−0.38**
Corn	September	0.00	**−0.11**	**−0.28**
Cotton	June	0.01	−0.02	−0.05
Cotton	July	0.01	−0.05	**−0.21**
Cotton	August	−0.04	**−0.11**	**−0.22**
Cotton	September	**−0.07**	**−0.14**	**−0.15**
Oats	May	−0.01	**−0.04**	**−0.04**
Oats	June	**−0.07**	**−0.13**	**−0.16**
Oats	July	**−0.08**	**−0.13**	**−0.25**
Peanuts	June	−0.06	**−0.10**	**−0.17**
Peanuts	July	−0.03	**−0.12**	**−0.23**
Peanuts	August	−0.05	**−0.21**	**−0.33**
Peanuts	September	**−0.10**	**−0.21**	**−0.25**
Sorghum	July	−0.02	**−0.11**	**−0.52**
Sorghum	August	**−0.14**	**−0.28**	**−0.60**
Sorghum	September	**−0.11**	**−0.22**	**−0.57**
Soybeans	June	0.03	**−0.06**	**−0.12**
Soybeans	July	0.00	−0.04	**−0.29**
Soybeans	August	−0.04	**−0.08**	**−0.31**
Soybeans	September	0.01	**−0.08**	**−0.26**
Spring wheat	June	**−0.10**	**−0.16**	**−0.23**
Spring wheat	July	**−0.11**	**−0.14**	**−0.17**
Spring wheat	August	−0.08	−0.08	**−0.16**
Winter wheat	April	0.00	−0.02	**−0.06**
Winter wheat	May	−0.03	**−0.08**	**−0.12**
Winter wheat	June	−0.04	**−0.10**	**−0.17**

Table 3. Mean CCIndex delta from the first reporting week to the final reporting week of the growing season for each crop and epoch.

Crop	HIST	MID45	MID85	END85
Barley	−0.09	−0.03	−0.01	−0.09
Corn	−0.10	−0.14	−0.17	−0.25
Cotton	−0.15	−0.23	−0.27	−0.24
Oats	−0.02	−0.09	−0.11	−0.23
Peanuts	−0.10	−0.13	−0.21	−0.18
Sorghum	−0.14	−0.22	−0.25	−0.20
Soybeans	−0.22	−0.24	−0.23	−0.36
Spring wheat	−0.14	−0.12	−0.06	−0.08
Winter wheat	−0.03	−0.07	−0.11	−0.14

increasing variability implies less predictable growing season conditions, which may increase the frequency of both short-term stress episodes and abrupt declines in crop condition during sensitive developmental windows.

Between END85 and HIST, increases in CCIndex variability are larger and more consistent across commodities than during MID, with mean standard deviation departures peaking in July at 0.07. Overall, 94% of crop-month combinations increase in CCIndex variability during END85, with six of these statistically significant. Barley, oats, spring wheat, corn, and soybeans are among the most consistently impacted crops through the growing season, with increasing CCIndex variability increases of

Table 4. Monthly mean CCIndex standard deviation deltas for each epoch (MID45, MID85, and END85) relative to HIST. Bold font indicates statistical significance at the 0.05 significance level.

Crop	Month	ΔMID45	ΔMID85	ΔEND85
Barley	June	**−0.06**	0.04	0.03
Barley	July	0.01	0.05	**0.08**
Barley	August	−0.02	0.04	0.05
Corn	June	0.00	0.04	0.04
Corn	July	0.00	0.06	**0.08**
Corn	August	−0.03	0.03	0.07
Corn	September	0.01	0.02	0.04
Cotton	June	−0.02	−0.01	0.02
Cotton	July	−0.03	−0.04	0.01
Cotton	August	0.01	−0.01	0.02
Cotton	September	−0.01	−0.03	−0.04
Oats	May	0.01	0.03	0.03
Oats	June	0.03	**0.07**	**0.07**
Oats	July	0.01	0.06	**0.09**
Peanuts	June	−0.04	−0.05	0.01
Peanuts	July	0.01	−0.01	0.05
Peanuts	August	−0.01	−0.06	0.02
Peanuts	September	−0.03	−0.04	**−0.06**
Sorghum	July	0.05	0.08	0.13
Sorghum	August	−0.01	−0.03	0.02
Sorghum	September	0.03	0.01	0.02
Soybeans	June	−0.02	0.02	0.03
Soybeans	July	−0.02	0.04	0.07
Soybeans	August	−0.03	0.04	0.03
Soybeans	September	−0.04	0.02	0.01
Spring wheat	June	−0.02	0.10	**0.09**
Spring wheat	July	0.02	0.05	**0.08**
Spring wheat	August	0.00	−0.02	0.00
Winter wheat	April	0.00	−0.01	0.01
Winter wheat	May	−0.02	0.00	0.00
Winter wheat	June	−0.02	0.03	0.01

0.07–0.09. Directional consistency across future epochs underscores the heightened risk of shifting crop conditions under future climate scenarios, as from MID85 to END85, 71% of crop-month combinations retain the same sign of variability change—a continued intensification of interannual volatility. Among the small subset of combinations that suggest a decline in condition variability under MID85, eight of the ten transition to increasing variability under END85. In terms of crop condition extremes, CCIndex values corresponding to the 10th percentile under HIST consistently align with higher percentiles under END85, commonly between the 25th and 55th percentiles (figure 4). Overall, crop conditions considered extremely low during HIST increasingly resemble typical growing-season outcomes by the late twenty-first century. At the upper end of the distribution, CCIndex values near the 90th percentile during HIST commonly shift toward the 98th percentile under END85, suggesting a relative reduction in the frequency of exceptionally favorable condition outcomes.

3.2. Spatial patterns of annual crop condition change

To evaluate spatial patterns of projected CCIndex change, annual mean deltas were examined at the state level for each crop and emissions scenario relative to HIST. These spatial patterns reveal pronounced regional and crop-specific differences in projected mid- and late-century crop condition responses (figures 5–7). Under MID45, annual mean CCIndex departures from HIST are mixed and generally subtle, with weak and spatially inconsistent signals of degradation (figure 5). Among all crops, barley, sorghum, and spring wheat undergo the largest annual CCIndex declines nationally, each with statistically significant reductions of $\leqslant -0.10$ relative to HIST (table 5), corresponding to good-to-excellent changes ranging from −7% to −1%. Soybeans are the only crop to experience nationally aggregated

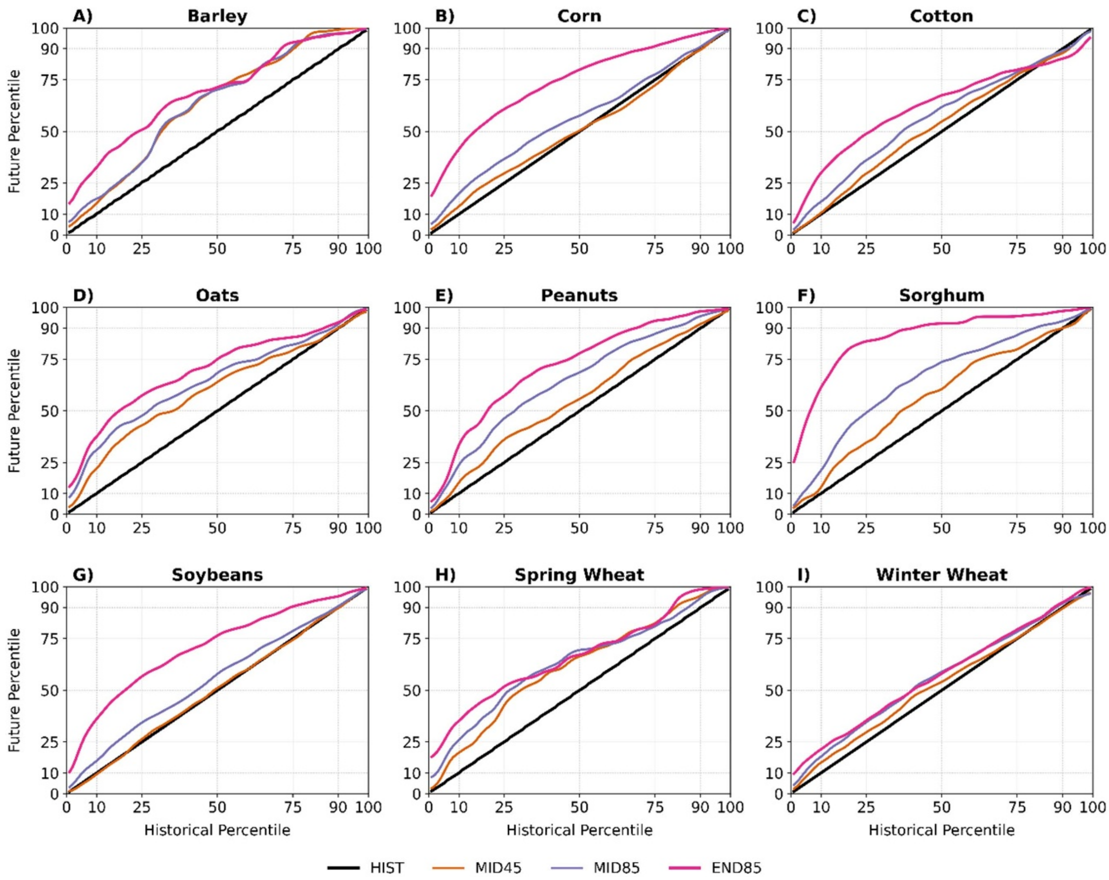

Figure 4. Percentile comparisons of HIST and future CCIndex distributions by crop. Curves above the HIST 1:1 line indicate lower future CCIndex values relative to the historical distribution.

increases in annual CCIndex ratings under MID45, albeit statistically insignificant. At the state level, statistically significant annual trends under MID45 are relatively uncommon; of the 94 state-crop combinations, only 20% exhibit statistically significant trends. Of those nineteen state-crop combinations, only four represent increases in crop conditions (Michigan winter wheat, California winter wheat and cotton, and Arizona cotton). Spatially, most of the statistically significant declines are concentrated among small grain crops (barley, oats, and spring wheat) across the northern tier of the conterminous U.S. Trends across the central U.S., including the Corn Belt and central Great Plains, are mostly mixed and insignificant for major commodities, including corn, soybeans, sorghum, and winter wheat. Across the Southern Plains and portions of the Southeast, several key crops—including corn, cotton, peanuts, sorghum, and winter wheat—undergo declining annual CCIndex trends under MID45, although only a subset of these trends reach statistical significance. Texas is notable, as all five crops cultivated within the state display declining annual CCIndex values under MID45, with magnitudes ranging from −0.02 to −0.24 and encompassing two of the top five most severe declining trends (good-to-excellent change of −1% to −10%).

The MID85 scenario produces a more robust and spatially coherent signal of annual crop condition deterioration (figure 6), consistent with patterns observed at the monthly scale. At the national level, conditions are projected to undergo statistically significant declines across all crops. Nationally, sorghum displays the strongest annual decline under MID85 (−0.21), followed by peanuts, barley, spring wheat, and oats (−0.16 to −0.10), while cotton, corn, winter wheat, and soybeans are projected to have more moderate declines (table 5; good-to-excellent change of −2% to −13% across all crops). State-level responses further highlight the strengthening of the MID85 degradation projection, with 33% of state-crop combinations yielding a statistically significant declining CCIndex trend relative to HIST. Similar to MID45, much of the statistical significance is concentrated among small grain crops (barley, oats, and spring wheat) across the northern U.S., as well as cropping systems across the Southern Plains and Southeast (corn, cotton, peanuts, sorghum, and winter wheat). Texas, together with much of the broader Great Plains region, emerges as a focal area of declining CCIndex ratings under MID85. For Texas, all evaluated crops exhibit statistically significant annual CCIndex declines ranging from −0.14 to −0.35,

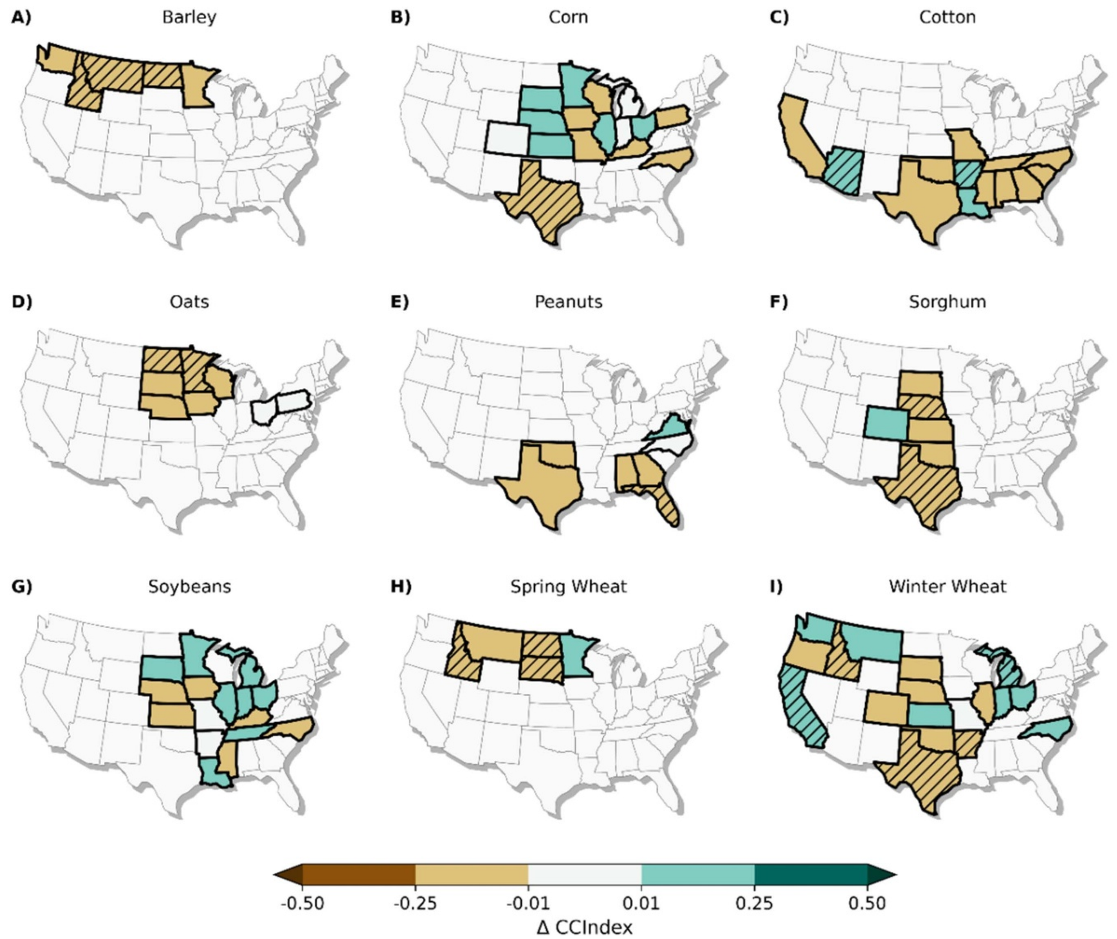

Figure 5. Annual mean CCIndex deltas for MID45 relative to HIST by state-crop combination. Hatching indicates statistical significance at the 0.05 level.

making it the only state where declines are statistically significant across all commodities. For corn and soybeans, annual CCIndex changes across the core Midwest production region indicate widespread but subtle annual CCIndex declines (−0.04 to −0.13), with only a small number of northern and eastern fringe Midwest states having slight and statistically insignificant improvements. Barley stands out as the crop for which all producing states are projected to experience declining annual CCIndex values under MID85, while at least 80% of states contain declining conditions for all remaining crops.

During END85, nationally aggregated annual CCIndex trends intensify substantially across all crops examined, yielding a strong and spatially coherent signal of late-century condition deterioration (figure 7). Crop condition changes between END85 and HIST are statistically significant for all nine crops analyzed at the national level. Of the nine crops, sorghum is projected to experience the most robust decline (−0.57), followed by corn (−0.29), with soybeans, spring wheat, peanuts, and barley also having strong declines ranging from −0.19 to −0.24 (table 5; good-to-excellent change of −4% to −34% across all crops). State-level responses further underscore the severity of late-century crop condition impacts, as 93% of state-crop combinations are projected to experience declining annual CCIndex values, with 85% of these declines statistically significant. Regionally, the Great Plains is projected to be the most affected under high-emission scenarios, with END85 annual CCIndex reductions across major commodities (corn, cotton, oats, peanuts, sorghum, soybeans, spring wheat, and winter wheat). Among all crops, winter wheat is the only crop for which fewer than 50% of producing states contain statistically significant declining trends. Nevertheless, when aggregated nationally, the END85 scenario consistently indicates widespread crop condition deterioration across the U.S.

3.3. Changes in interannual crop condition variability

Like mean CCIndex ratings and standard deviations at the monthly level, strong inverse relationships are present for annual, state-level crop conditions, indicating that projected declines in mean crop conditions are accompanied by increases in year-to-year variability for most state-crop combinations. Furthermore, the strength of the inverse correlation between CCIndex variability deltas and mean CCIndex deltas increases from MID45 to MID85 to END85 across most commodities, reflecting growing interannual

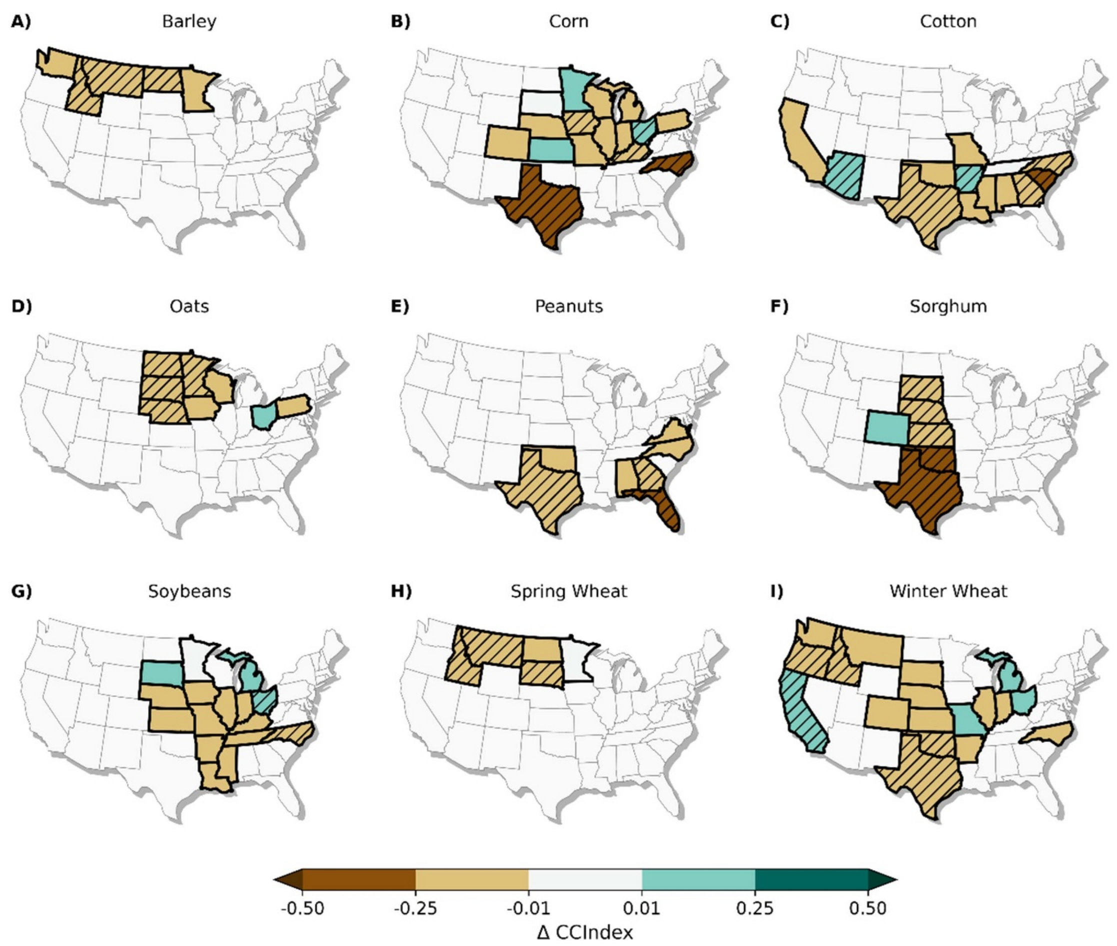

Figure 6. As in figure 5, but for annual mean CCIndex deltas between MID85 and HIST.

Table 5. Annual, national mean CCIndex rating deltas and standard deviation deltas for each epoch (MID45, MID85, and END85) relative to HIST. Bold font indicates statistical significance at the 0.05 significance level.

	MID45		MID85		END85	
	ΔCCIndex	ΔCCIndex σ	ΔCCIndex	ΔCCIndex σ	ΔCCIndex	ΔCCIndex σ
Barley	**−0.12**	−0.02	**−0.13**	0.01	**−0.23**	**0.07**
Corn	−0.02	0.01	**−0.07**	**0.04**	**−0.29**	**0.04**
Cotton	−0.02	0.02	**−0.08**	0.05	**−0.16**	**0.15**
Oats	**−0.05**	**0.04**	**−0.1**	**0.06**	**−0.15**	**0.09**
Peanuts	−0.06	0.02	**−0.16**	0.02	**−0.24**	0.01
Sorghum	**−0.10**	0.01	**−0.21**	0.02	**−0.57**	0.03
Soybeans	0.00	−0.02	**−0.06**	0.02	**−0.24**	0.02
Spring wheat	**−0.10**	−0.01	**−0.13**	**0.05**	**−0.19**	**0.09**
Winter wheat	−0.03	**0.04**	**−0.07**	**0.05**	**−0.11**	**0.06**

instability as baseline conditions deteriorate. Under MID45, variability trends remain relatively weak and spatially inconsistent, as 51% of state-crop combinations increase in CCIndex variability relative to HIST, with only 7% of these increases statistically significant (figure 8). Nationally, oats and winter wheat are projected to be the only crops to undergo a statistically significant increase in CCIndex variability (0.04; a good-to-excellent equivalent of 2%), whereas all other crops exhibit statistically insignificant variability changes under MID45 (table 5). At the state level, oats experience the most coherent variability response under MID45, with nearly all oat-producing states increasing their CCIndex variability. In contrast, several crops concentrated in the Southwest, Southern Plains, and Southeast (corn, cotton, peanuts, and soybeans) suggest subtle declining variability during MID45. Therefore, these decreases in CCIndex variability suggest a transition toward more consistently degraded crop conditions rather than increased interannual fluctuations across much of the southern U.S. under MID45.

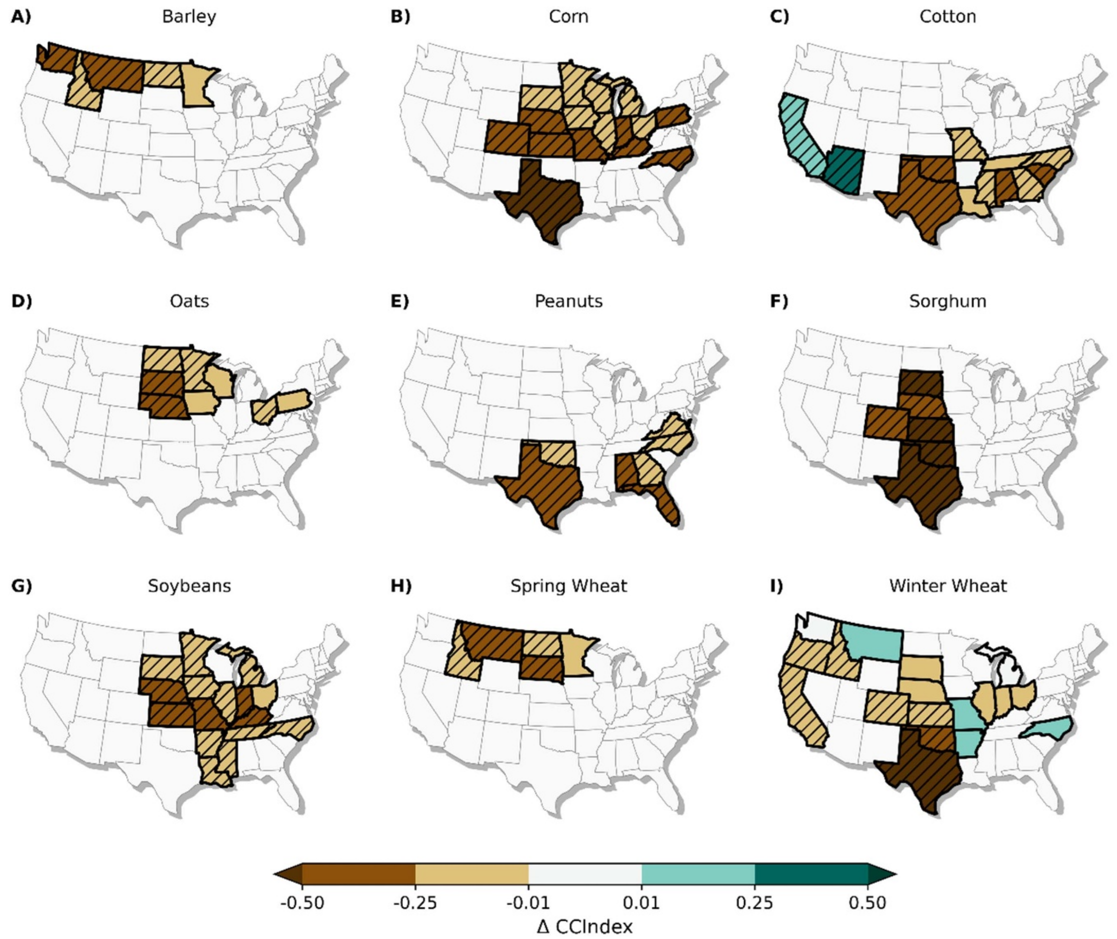

Figure 7. As in figure 5, but for annual mean CCIndex deltas between END85 and HIST.

Greater spatial coherence in CCIndex variability trends emerges under the MID85 scenario (figure 9). At the national level, oats and winter wheat continue to increase in variability, reaching 0.06 and 0.05, respectively, while all remaining crops undergo an increase under MID85 of at least 0.01 (good-to-excellent changes ranging from 1% to 4%). Under MID85, 61% of state-crop combinations experience an increase in CCIndex variability, with only one of these increases statistically significant. Regionally, major row crops in states across the Midwest and small grain crops of the northern U.S. generally increase in variability, becoming more spatially consistent under MID85, whereas variability patterns among crops in the Great Plains and broader southern U.S. differ. For example, sorghum exhibits declining variability across southern portions of the region but increasing variability farther north, while winter wheat displays broader, increasing CCIndex variability across the Great Plains and extending into the Northwest. Still, across much of the broader southern U.S., declining variability remains the dominant signal under MID85, reinforcing the interpretation that crop conditions in these regions shift toward more uniformly poorer outcomes rather than increased exposure to episodic extremes. However, regions with both declining mean CCIndex values and increasing interannual variability may face a dual risk—poorer average crop conditions and greater uncertainty in year-to-year production outcomes.

By END85, CCIndex variability trends intensify and become more spatially extensive across nearly all crops and production regions (figure 10). Like MID85, no crop examined in this study experiences a decrease in CCIndex variability at the national level during END85 relative to HIST. Cotton undergoes the most robust increase in CCIndex standard deviation at 0.15, followed by oats and spring wheat at 0.09 each (good-to-excellent changes ranging from 4% to 9%). In total, 72% of state-crop combinations increase in CCIndex standard deviation, with 18% of these statistically significant and mostly confined to the Great Plains. Similar to MID85, Midwest row crops (corn and soybeans) and northern U.S. small grain crops (spring wheat, oats, and barley) undergo stronger and more widespread increases in interannual CCIndex variability. Additionally, Great Plains and southern U.S. cropping systems experience weaker spatial coherence by END85, characterized by a mixture of increasing and decreasing variability across states.

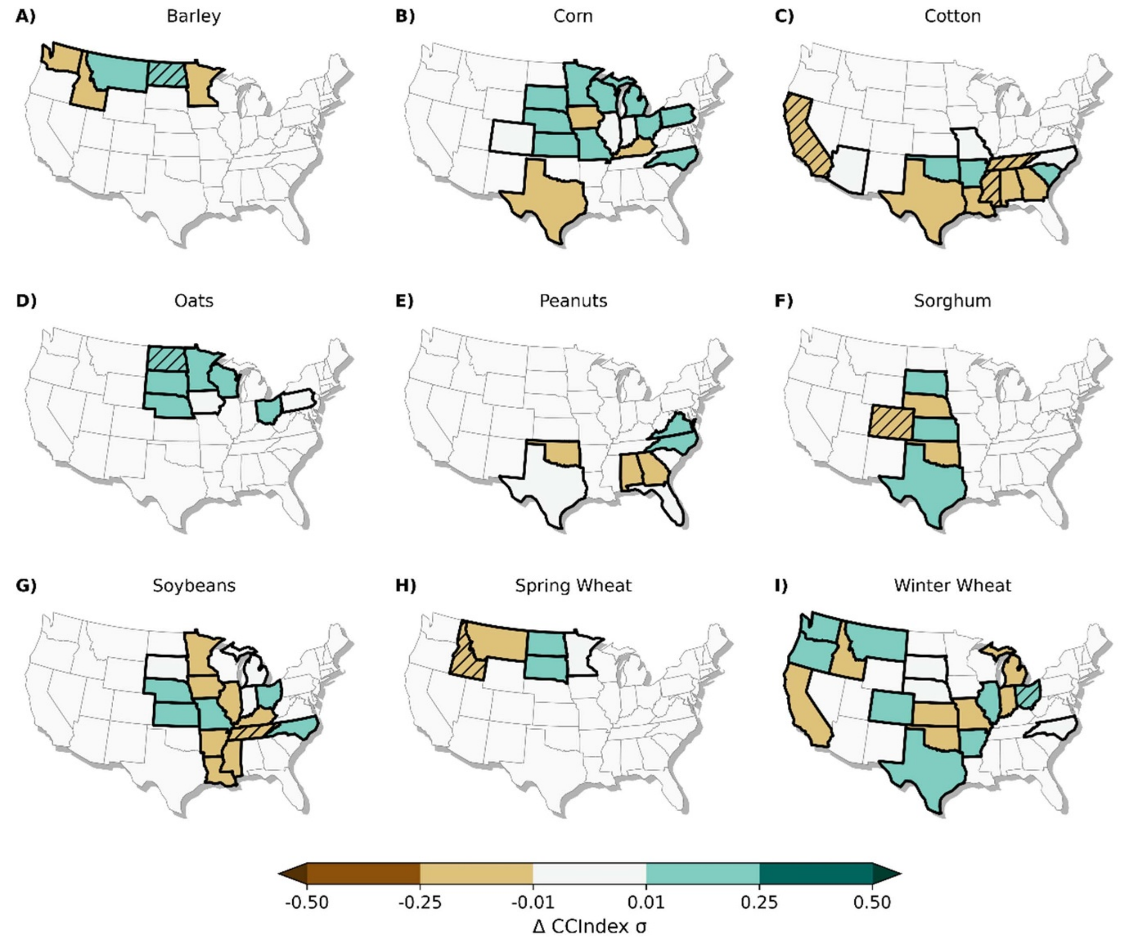

Figure 8. Annual CCIndex standard deviation deltas for MID45 relative to HIST by state-crop combination. Hatching indicates statistical significance at the 0.05 level.

4. Discussion

4.1. Phenology and climate stressors

The timing and magnitude of projected twenty-first-century deterioration in crop conditions are agronomically critical, as the largest negative departures align with phenological windows when physiological stress exerts a disproportionate influence on final yield outcomes (figure 3; Bundy *et al* 2024). The phenology-climate linkage provides a foundation for interpretation, as the explanatory relationships between the primary climate predictors used in this study and the CCIndex are both crop- and region-dependent, reflecting differences in baseline climate, management practices, and the alignment of climate stress with sensitive developmental stages. Consequently, even subtle changes in seasonal climate can translate into noteworthy condition changes if they occur during periods of heightened physiological sensitivity (Westcott and Jewison 2013).

Across most crops examined in this study, the seasonal structure of condition change is generally coherent within each epoch. During both MID and END, statistically significant projected condition declines are most prominent during the latter half of the growing season (July–September), while early-to mid-season periods (May–July) are characterized primarily by increases in condition variability rather than consistent mean declines (figure 3). This distinction is nontrivial, as increasing condition variability during early vegetative stages elevates the probability of poorer starts (e.g. uneven emergence, early-season stress, or replanting), whereas systematic condition declines later in the summer growing season indicate a trend toward more frequent or more intense stress during reproductive stages. Therefore, this crop condition outlook is not simply 'worse on average;' rather, it suggests a growing season that becomes increasingly volatile early and increasingly unfavorable during the months that most directly govern yield outcomes.

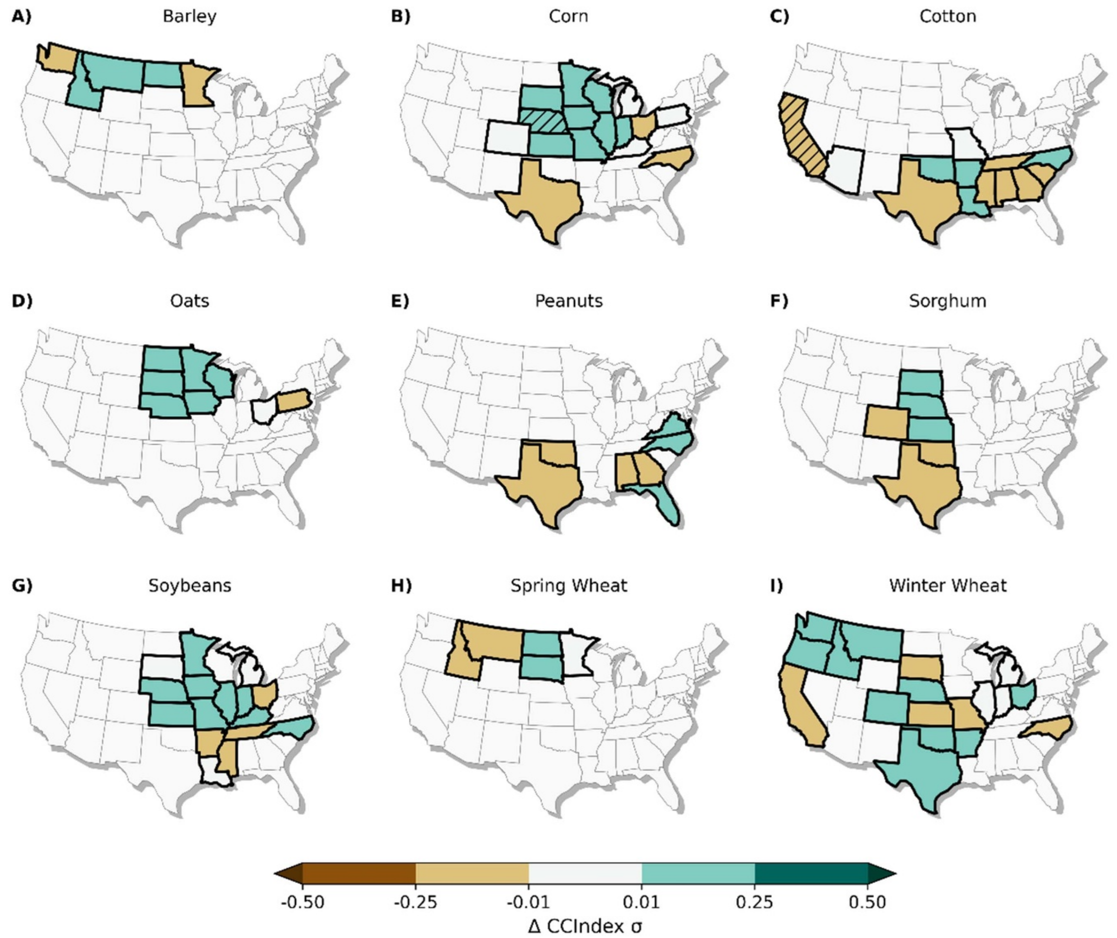

Figure 9. As in figure 8, but for annual CCIndex standard deviation deltas between MID85 and HIST.

The phenological interpretation of this projected seasonal contrast is consistent across major U.S. production regions. For northern U.S. small grains (barley, oats, and spring wheat), early-season condition variability overlaps with stem elongation through booting and heading when rapid canopy expansion and reproductive primordia development increase sensitivity to short-term heat and moisture stress (Slafer and Rawson 1994, Porter and Gawith 1999, Alghabari *et al* 2014, U.S. Department of Agriculture, National Agricultural Statistics Service 2016). For Midwest U.S. row crops (corn and soybeans), May and June correspond to stand establishment and early vegetative growth, during which episodic temperature extremes, oversaturated soils, and precipitation intermittency can increase the risk of uneven emergence and reduce early canopy vigor (Schlenker and Roberts 2009, Hatfield and Prueger 2015, Kaur *et al* 2017). In the more diverse southern U.S. production systems, phenological alignment varies by crop: sorghum transitions from emergence into vegetative growth (Gerik *et al* 2024), cotton progresses from establishment into early squaring (Zonta *et al* 2017), and peanuts advance from early vegetative growth toward initial flowering (Boote 1982). Winter wheat is an exception, as its most sensitive reproductive stages (heading, flowering, and early grain fill) often peak in May and June (Bruns and Croy 1983), coinciding with the period when summer crops remain mostly in their vegetative stages.

These phenology-specific responses occur in a climate characterized by progressively warmer conditions, with projected mean temperatures increasing from mid-century to late-century and becoming most pronounced under the high-emissions scenario (supplemental figure 6), trends similarly projected in previous climate analyses (e.g. Vose *et al* 2017, Almazroui *et al* 2021). Additionally, rising temperatures increase vapor pressure deficit and evaporative demand, enhancing crop water loss and increasing the probability that soil moisture becomes limiting even in the absence of large changes in seasonal precipitation (Wilson *et al* 2023). Precipitation projections during the vegetative phases of summer crop development indicate decreases in regional monthly mean precipitation of 4% during MID45, 15% during MID85, and 18% during END85 relative to HIST (supplemental figure 7). Trends in precipitation variability are regionally dependent, as the Midwest is projected to experience the most pronounced

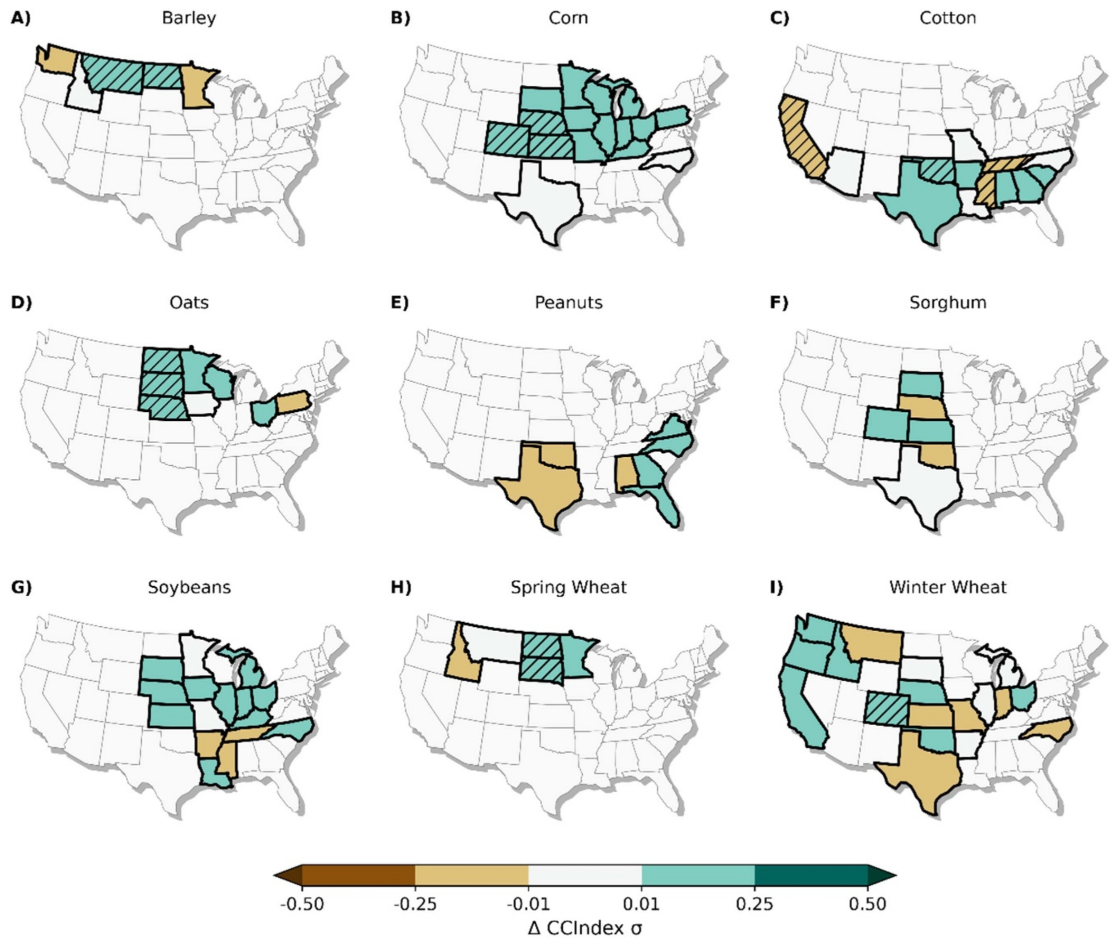

Figure 10. As in figure 8, but for annual CCIndex standard deviation deltas between END85 and HIST.

and consistent increases across future epochs, ranging from 10% to 26% relative to HIST (supplemental figure 7), consistent with previous studies (e.g. Chen and Ford 2023). Thus, this Midwest trend indicates more frequent dry spells punctuated by heavy precipitation events—an ongoing regional trend over the past several decades (Easterling *et al* 2018, Changnon and Gensini 2019, Chen and Ford 2023, Na and Najafi 2024). This combination plausibly produces the projected pattern of mean condition declines coupled with increases in condition variability as dry intervals can rapidly amplify moisture stress under elevated evaporative demand (Walthall *et al* 2012, Bolster *et al* 2023), while heavy precipitation events can induce waterlogging, runoff, disease pressure, and nutrient loss, particularly in poorly drained soils (Li *et al* 2019).

Climate volatility becomes especially consequential as crops enter reproductive stages, which coincide with the period of strongest projected mean CCIndex decline (July–September; figure 3). Physiologically, this period is important because reproductive development is highly sensitive to short-duration heat and moisture stress, reducing crop quality and yield potential (Walthall *et al* 2012). Elevated temperatures can reduce pollen viability, disrupt fertilization, and increase flower or pod abortion, while soil moisture deficits can limit transpiration, reduce canopy cooling, and accelerate stress during periods of high evaporative demand. When heat and moisture stress persist into grain- or seed-filling periods, crops may also experience shortened filling duration, reducing the time available for biomass accumulation and yield formation. For corn, this window encompasses tasseling, silking, and early grain fill; for soybeans, flowering through pod set and seed fill—stages well known to be highly sensitive to heat and water deficits (Lauer 2012, Westcott and Jewison 2013, Mourtzinis *et al* 2015). Northern U.S. small grains are commonly in flowering and grain fill during mid-summer, while in southern U.S. systems, sorghum progresses through heading, flowering, and grain fill; cotton through boll set and early boll fill; and peanuts through pegging and early pod fill (USDA 2016).

Many U.S. regions are projected to experience a crossing of critical temperature levels, including thresholds near ∼30 °C that have been associated with reduced pollen viability, fertilization efficiency, and pod retention in major row crops (supplemental figure 6; Hatfield and Prueger 2015). Regional monthly mean temperatures also continue to rise during July, August, and September, with the strongest late-summer warming projected under END85 relative to HIST (supplemental figure 6). Additionally, each production region undergoes some degree of a decrease in mean monthly precipitation during crop reproductive stages, with mean regional decreases of 8% during MID45, 14% during MID85, and 23% during END85 relative to HIST (supplemental figure 7). Therefore, the compounding heat-moisture stress points toward a mid- to late-summer stress regime that can rapidly degrade crop conditions and, consequently, crop yield prospects (figure 3).

Beyond temperatures and precipitation, the projected evolution of severe convective storm environments provides an additional pathway for growing season condition risk through wind and hail damage, especially across the Midwest and other thunderstorm-prone, agriculturally dominant regions. Projected increases in environments supportive of supercells (Ashley *et al* 2023), large hail (Gensini *et al* 2024), and high-impact derechos (Lasher-Trapp *et al* 2023, Kaminski *et al* 2025) imply a compounding hazard backdrop during peak canopy development and reproductive exposure. While USDA NASS crop condition surveys integrate multiple stress signals and may not explicitly isolate storm damage, severe convective events can produce abrupt weekly condition declines (e.g. the 10 August 2020 Iowa derecho; Bundy *et al* 2026a) and heightened interannual variability. Thus, such events offer a plausible physical mechanism linking projected changes in convective storm environments to episodic in-season crop condition declines and increased interannual variability.

4.2. Yield implications

Projected declines in CCIndex ratings indicate that a smaller proportion of cropland is expected to be rated in good or excellent condition, which are categories associated with yield prospects that are normal to above normal (USDA 2016). Correspondingly, declining CCIndex ratings imply an increasing portion of crops rated in fair, poor, or very poor condition, thereby increasing the probability of below-normal yield outcomes as the twenty-first century progresses. This interpretation is consistent with established empirical relationships between in-season condition ratings and end-of-season yield outcomes, and it also aligns with observed condition changes since 1986 for some regions. Over the historical crop-condition observation period (since 1986), the most robust and statistically significant declines in U.S. crop conditions have been concentrated across the Great Plains, with trend magnitudes exceeding -0.01 CCIndex yr^{-1} in many states (Bundy *et al* 2024). For other regions, such as the Midwest, crop condition trends from 1986 through 2022 were generally mixed, lacking spatial continuity across crops and states (Bundy *et al* 2024). A similar pattern is projected for intermediate scenarios during the mid-century before continued degradation under high-emissions scenarios during both the mid- and late centuries (figures 5–7). Meanwhile, the only region with statistically significant improvements in crop conditions was across the Delta and Southeast throughout the historical period (Bundy *et al* 2024), which is projected to eventually experience a trend reversal, especially across the Southeast region (figures 5–7).

The seasonal timing of declining crop conditions further supports a yield-risk interpretation, as the strongest deterioration on average is projected to occur during mid- to late-summer, when heat and moisture stress exert the strongest control on reproductive success and final yield formation. Consistent with this sensitivity, the empirical relationship between USDA crop condition ratings and yield indicates that conditions from July onward explain up to about 85% of national barley, corn, and soybean yield variability; about 80% for sorghum and spring wheat; 70% for winter wheat; near 55% for oats and peanuts; and close to 40% for cotton (Irwin and Good 2017a, 2017b, Irwin and Hubbs 2018a, 2018b, Bundy *et al* 2024). This highlights the tight coupling between condition anomalies during peak stress windows and realized yield outcomes. Therefore, with most crops projected to undergo crop condition degradation at the national level, especially under pessimistic emission scenarios, and given the strong explanatory power between the CCIndex and national-level yield variance, the probability of below-normal yield outcomes is likely to increase through the twenty-first century.

This interpretation using crop condition ratings broadly aligns with the direction of previous yield projection studies, particularly the tendency toward increasingly negative mid- to late-century outcomes for corn and other heat-sensitive crops under high-emission pathways, while some responses are scenario- and assumption-dependent (e.g. Walthall *et al* 2012, Huntington *et al* 2020, Waldhoff *et al* 2020, Lin *et al* 2021, Fei *et al* 2023). Statistical and empirical yield studies have repeatedly demonstrated that exposure to high temperatures during reproductive and grain-filling periods has a disproportionate negative effect on major U.S. crops (e.g. Schlenker and Roberts 2009, Lobell *et al* 2014, Tack *et al* 2015, Waldhoff *et al* 2020), while process-based modeling studies similarly identify heat stress, soil moisture deficits, and precipitation variability as key drivers of future yield risk (e.g. Rosenzweig *et al* 2014, Schauberger *et al* 2017, Fei *et al* 2023). This analysis complements prior literature by focusing on in-season USDA crop condition ratings rather than end-of-season yield alone. Additionally, while elevated CO_2 can enhance photosynthesis and can result in yield gains in controlled experiments, heat and drought stress negate or outweigh these benefits, and thus, yield outcomes are constrained by the adverse effects of climate (Rezaei *et al* 2023, Ainsworth *et al* 2025). Even studies that explicitly incorporate adaptation indicate net yield losses for key staple crops under climate change, emphasizing that adaptation can buffer but does not eliminate yield risk (Hultgren *et al* 2025). Within the U.S.-focused literature, projected losses are consistently greatest in the Southern Plains and broader Great Plains (Walthall *et al* 2012, Kukal and Irmak 2018), patterns that align with those emerging from crop condition projections.

4.3. Mitigation and adaptation

Although observed crop conditions since 1986 have not mirrored yield trends directly, the projected evolution of crop conditions under future climate scenarios suggests increasing risk of deteriorating conditions if adaptation does not advance sufficiently. Effective responses will be region- and crop-specific, as no single strategy can address the diversity of production systems, climate stressors, and producer needs across the U.S. (IPCC, 2022). Management practices that buffer heat and moisture stress during critical reproductive windows are likely to provide some of the largest benefits, including adjustments to planting dates, cultivar or hybrid selection, improved soil-water conservation, and more efficient irrigation scheduling where water resources and infrastructure allow (Sacks and Kucharik 2011, Lobell and Gourdji 2012, Hatfield and Prueger 2015, Basche *et al*, 2017). Cultivar and hybrid adaptation may be especially important where projected warming increases exposure to reproductive-stage stress, including selection for heat and drought tolerance, improved reproductive resilience, and phenological traits that avoid peak summer stress. Altered planting windows could further reduce risk by shifting sensitive reproductive stages away from periods of maximum heat and evaporative demand, although this strategy may be constrained by spring field conditions, frost risk, crop insurance dates, and regional management calendars. Precision agriculture tools, including soil moisture monitoring, remote sensing, variable-rate irrigation, and within-field stress detection, may also help producers identify emerging stress earlier and target management responses more efficiently.

Soil-focused adaptation strategies may further buffer projected climate impacts by improving infiltration, soil structure, and plant-available water. Practices such as cover cropping, residue management, prairie or field-edge buffering, and diversified crop rotations can increase soil resilience and help offset stress associated with higher evaporative demand and precipitation variability (Schulte *et al* 2017, Hatfield and Dold 2019, Bolster *et al* 2023, Sutton *et al* 2025). However, adaptation through irrigation is constrained by water availability and the long-term sustainability of groundwater resources. For instance, across the Southern Plains, a region characterized by historically declining crop conditions (Bundy *et al* 2024) and a projected continuation of crop condition declines (figures 5–7), marginal biophysical characteristics require ample irrigation, yet persistent groundwater declines in the Ogallala Aquifer limit the extent to which irrigation can serve as an unlimited buffer (McGuire 2017). This groundwater constraint introduces a structural ceiling on resilience in portions of the Southern Plains and suggests that feasible adaptation may require more fundamental transitions, including shifts in cropping systems, acreage reallocation, and optimization of deficit irrigation strategies (Scanlon *et al* 2012, Chai *et al* 2016, Deines *et al* 2019).

Crop condition projections also underscore the need for risk communication and policy frameworks that emphasize variability and the risk of more frequent extreme conditions, rather than changes in mean conditions alone. A future in which historically poor crop conditions become more typical and exceptionally favorable conditions become increasingly rare has direct implications for crop insurance, disaster assistance programs, grain reserve planning, and commodity market stability (Hatfield *et al* 2011, FAO 2018, IPCC 2022, Glauber 2023).

4.4. Limitations and future work

Several limitations should be considered when interpreting crop condition projections. First, USDA CPCR data, while widely used and valuable for agricultural monitoring, are based on subjective assessments and may be influenced by observer interpretation (Beguería and Maneta 2020). USDA NASS applies multi-stage quality control procedures to improve consistency across weeks, states, and years; however, changes in observer experience, survey participation, interpretation of condition categories, or reporting practices could still affect temporal consistency. In addition, CPCR data do not explicitly distinguish between irrigated and rainfed production systems, double-cropping practices, soil-quality classes, or specific management systems (Irwin and Good 2017b). Therefore, results should be interpreted as climate-driven signals within the available USDA crop condition record, while recognizing that some portion of historical variability may reflect reporting uncertainty or changes in observer composition.

Despite these limitations, CPCR-based analyses remain useful for evaluating seasonal crop condition tendencies and long-term agricultural risk patterns (Bundy *et al* 2024, 2025b).

A second limitation is that the modeling framework is designed to estimate the climate-driven component of CCIndex variability rather than provide a complete causal representation of all agronomic influences. Crop condition and yield are affected by numerous non-climate factors, including pest pressure, disease outbreaks, nutrient availability, cultivar and hybrid selection, planting and harvest timing, irrigation access, soil quality, drainage, and market-driven management decisions. These factors can modulate crop sensitivity to heat, precipitation variability, and moisture stress, and their omission may influence the magnitude of projected CCIndex changes. However, because USDA CPCR data are aggregated at the state level and do not identify the management systems, irrigation status, soil classes, or cultivar types associated with reported conditions, including such controls would require assumptions that could introduce additional uncertainty or misleading precision. As a result, projections are best interpreted as climate-conditional estimates of future crop condition risk, holding management, technology, soil conditions, irrigation, and adaptation implicitly constant relative to the historical baseline.

A third limitation is that future projections are based on a single dynamically downscaled regional climate simulation. WRF-BCC provides a physically consistent, high-resolution representation of future climate conditions over the U.S., but it does not quantify the full range of uncertainty associated with internal climate variability, global climate model structure, regional model configuration, or model-specific bias. Therefore, CCIndex projections should be interpreted as one plausible high-resolution realization of climate-driven crop condition risk rather than as a probabilistic projection or ensemble mean. The spatial coherence and consistency of projected changes across epochs and emissions scenarios support the interpretation of increasing climate-related crop stress, but the precise magnitude of projected changes should be interpreted with caution. Importantly, reliance on a single climate model does not invalidate the analysis; rather, it frames the results as a scenario-based assessment that links USDA crop condition responses with detailed regional climate information at spatial and temporal scales relevant for agricultural stress.

Finally, although XGBoost provides flexibility for modeling nonlinear crop–climate relationships, interpretability limitations should be acknowledged. Feature importance metrics and partial dependence plots can identify influential predictors and broad response patterns, but they should not be interpreted as fully causal explanations of crop condition change. Many predictor variables are physically related, and collinearity can influence how importance is distributed across variables. In addition, interactions among climate predictors and the absence of explicit non-climate controls limit the extent to which individual model responses can be attributed to a single driver. Therefore, model interpretation is focused on identifying dominant climate associations and projection patterns rather than isolating complete causal mechanisms.

Future research could strengthen this framework by using multi-model regional climate ensembles or additional downscaled CMIP simulations, which would allow uncertainty bounds to be quantified more directly and would help test the robustness of projected crop condition responses across alternative climate futures. Linking crop condition observations with spatially explicit soil, irrigation, cultivar, and management datasets could help separate climate-driven risk from management-mediated outcomes where such information can be reliably paired with reported crop conditions. Finer spatial analyses within states could also improve identification of localized climate and yield risks. In addition, translating CCIndex projections into decision-relevant metrics, such as the probability of falling below critical condition thresholds, return periods of poor or very poor seasons, or potential insurance-relevant risk indicators, would improve applied interpretation. Despite the noted limitations, this study provides a useful climate-conditional framework for assessing how future climate conditions may alter state-scale patterns of U.S. crop condition risk and for identifying where additional monitoring and adaptation planning may be most needed.

5. Conclusion

Crop condition assessments throughout the growing season are critical for diagnosing agroclimatic impacts on crop development and anticipating yield outcomes, yet one of the most comprehensive and consistent records of in-season condition information—USDA NASS crop condition ratings—remains comparatively underused in climate-impact assessments. Leveraging historical crop condition ratings together with high-resolution, dynamically downscaled regional climate simulations across three 15-year epochs (HIST: 1990–2005; MID: 2040–2055; END: 2085–2100) provides a novel, stakeholder-relevant picture of how both the mean state and year-to-year variability of crop conditions may evolve across the U.S. Furthermore, crop condition projections offer actionable insight into when (which phenological stages), where (which production regions), and how (which climate stressors) future risk may change.

By using machine learning models across each state, month, and crop to predict crop condition ratings using a series of climate variables (e.g. precipitation totals, minimum and maximum temperatures, water balance estimates, and soil moisture proxies), multiple conclusions emerge about the potential future trajectory of nine major U.S. crops:

- Crop conditions are projected to decline relative to the historical period, with the magnitude of change progressing from MID45 to MID85 to END85 across most major commodities. The largest declines are concentrated from July onward, when most summer crops enter reproductive development and yield formation, indicating a reduced probability of crops rated in good or excellent condition during the most yield-sensitive portion of the growing season. This signal is consistent with increases in temperatures co-occurring with declining mean precipitation and greater precipitation intermittency, collectively favoring more frequent and/or more intense summer stress.
- Crop conditions are projected to become more variable at the national level across most crops, with peak increases in variability occurring during the late-vegetative to reproductive transition phase. Increasing volatility at this stage raises early- to mid-season uncertainty heading into the period that is closely linked to yield outcomes, implying greater year-to-year swings in crop prospects.
- Regional risk is best interpreted through the joint behavior of crop condition means and variability. Where declining mean conditions coincide with increasing interannual variability (e.g. among northern U.S. small grains and portions of Midwest row crops), the result is a compounding risk—a lower baseline state coupled with more frequent excursions into unfavorable seasons, thereby reducing predictability and reliability. Where decreasing mean conditions coincide with decreasing variance (mostly southern U.S. cropping systems), the signal instead implies a more uniform and persistent deterioration, consistent with a chronic downward shift in baseline climate suitability rather than amplified interannual swings.

These projections are intentionally framed from a climate perspective, as this provides a benchmark of risk if mitigation is insufficient and if adaptation does not keep pace through the twenty-first century. While targeted adaptation can reduce exposure to some extreme weather perils during much of the growing season, crop condition projections suggest that stress indicators and volatility could increasingly define U.S. production risk. For stakeholders, this work provides an interpretable early-warning framework for when condition risk occurs, where conditions deteriorate the most, and how climate stressors combine to increase the occurrence of unfavorable conditions. Together, crop condition projections carry practical consequences for producers, traders, insurers, and supply chains by increasing production uncertainty, price and hedging risk, and exposure to correlated shortfalls that can ripple into global food security. As climate change reshapes agricultural risk, such early-warning perspectives are likely to become essential for sustaining resilient global food systems, and these findings underscore that sustainability will depend not only on long-term trends but on the capacity to anticipate and adapt to increasing volatility in the agroclimatic system.

Acknowledgments

This research was supported by the National Science Foundation Awards 1637225 and 1800582 and National Oceanic and Atmospheric Administration Award NA22OAR4690645. The authors acknowledge high-performance computing support from Cheyenne (DOI: 10.5065/D6RX99HX) provided by NCAR's Computational and Information Systems Laboratory, sponsored by the National Science Foundation. Mid-century simulations were performed on the Comet supercomputer, which is hosted by the San Diego Supercomputer Center at the University of California, San Diego. This computational resource was made available by the Atmospheric River Program (Phases 2 and 3), which is supported by the California Department of Water Resources (Awards 4600013361 and 4600014294, respectively) and the U.S. Army Corps of Engineers Engineer Research and Development Center (Award USACE W912HZ-15-2-0019). We also acknowledge and thank Dr Michael Papka (ANL) for data storage and postprocessing assistance. This research used resources of the Argonne Leadership Computing Facility, which is a DOE Office of Science User Facility supported under Contract DE-AC02-06CH11357. We thank the anonymous reviewers for their constructive feedback that greatly enhanced the quality of the research.

Data availability statement

The historical crop condition data that support the findings of this study are openly available at the following URL/DOI: https://quickstats.nass.usda.gov. Climatological data are openly available at the following URL/DOI: https://prism.oregonstate.edu. Please contact the corresponding author if there is interest in the crop projections or WRF-BCC simulations.

Supplementary Material available at: https://doi.org/10.1088/2976-601X/ae885b/data1.

Author contributions

Logan R Bundy 0000-0003-0868-4307
Conceptualization (lead), Data curation (lead), Formal analysis (lead), Investigation (lead), Methodology (equal), Visualization (lead), Writing – original draft (lead), Writing – review & editing (equal)

Vittorio A Gensini 0000-0001-6362-9197
Funding acquisition (equal), Project administration (lead), Resources (lead), Software (lead), Supervision (equal), Validation (equal), Writing – original draft (supporting), Writing – review & editing (supporting)

Walker S Ashley 0000-0003-0816-3333
Funding acquisition (equal), Project administration (supporting), Supervision (supporting), Validation (supporting), Writing – original draft (supporting), Writing – review & editing (supporting)

Alex M Haberlie 0000-0001-9172-4028
Data curation (supporting), Methodology (supporting), Supervision (supporting), Validation (supporting), Writing – original draft (supporting), Writing – review & editing (supporting)

Allison C Michaelis 0000-0002-0793-5779
Data curation (supporting), Funding acquisition (supporting), Resources (supporting), Writing – original draft (supporting), Writing – review & editing (supporting)

David Changnon
Writing – original draft (supporting), Writing – review & editing (supporting)

References

Ainsworth E A, Sanz-saez A and Leisner C P 2025 Crops and rising atmospheric CO_2: friends or foes? *Phil. Trans. R. Soc. B* **380** 20240230
Alghabari F, Lukac M, Jones H E and Gooding M J 2014 Effect of R ht alleles on the tolerance of wheat grain set to high temperature and drought stress during booting and anthesis *J. Agron. Crop Sci.* **200** 36–45
Allen J T, Giammanco I M, Kumjian M R, Jurgen Punge H, Zhang Q, Groenemeijer P and Ortega K 2020 Understanding hail in the earth system *Rev. Geophys.* **58** e2019RG000665
Almazroui M, Islam M N, Saeed F, Saeed S, Ismail M, Ehsan M A and Barlow M 2021 Projected changes in temperature and precipitation over the United States, Central America, and the Caribbean in CMIP6 GCMs *Earth Syst. Environ.* **5** 1–24
Angel J *et al* 2018 Midwest *Impacts, Risks, and Adaptation in the United States: Fourth National Climate Assessment, Volume II* ed D R Reidmiller, C W Avery, D R Easterling, K E Kunkel, K L M Lewis, T K Maycock and B C Stewart (U.S. Global Change Research Program) pp 872–940
Ashley W S, Haberlie A M and Gensini V A 2023 The future of supercells in the United States *Bull. Am. Meteorol. Soc.* **104** E1–E21
Bain R and Fortenbery T R 2017 Impact of crop condition reports on national and local wheat markets *J. Agric. Appl. Econ.* **49** 97–119
Basche A D and Edelson O F 2017 Improving water resilience with more perennially based agriculture *Agroecol. Sustain. Food Syst.* **41** 799–824
Beguería S and Maneta M P 2020 Qualitative crop condition survey reveals spatiotemporal production patterns and allows early yield prediction *Proc. Natl Acad. Sci. USA* **117** 18317–23
Bolster C H *et al* 2023 Agriculture, food systems, and rural communities *Fifth National Climate Assessment* ed A R Crimmins, C W Avery, D R Easterling, K E Kunkel, B C Stewart and T K Maycock (U.S. Global Change Research Program) ch 11 (https://doi.org/10.7930/NCA5.2023.CH11)
Boote K J 1982 Growth stages of peanut (Arachis hypogaea L.) *Peanut Sci.* **9** 35–40
Brimelow J C, Burrows W R and Hanesiak J M 2017 The changing hail threat over North America in response to anthropogenic climate change *Nat. Clim. Change* **7** 516–22
Brown M B and Forsythe A B 1974 Robust tests for the equality of variances *J. Am. Stat. Assoc.* **69** 364–7
Bruns H A and Croy L I 1983 Key developmental stages of winter wheat, Triticum aestivum *Econ. Bot.* **37** 410–7
Bruyère C L, Done J M, Holland G J and Fredrick S 2014 Bias corrections of global models for regional climate simulations of high-impact weather *Clim. Dyn.* **43** 1847–56
Bundy L R and Gensini V A 2022 An assessment of USDA corn condition ratings across the US Corn Belt *Agron. J.* **114** 601–17

Bundy L R, Gensini V A and Ashley W S 2025a United States pasture and rangeland conditions: 1995–2022 *Agron. J.* **117** e21736

Bundy L R, Gensini V A, Ashley W S and Haberlie A M 2025b On the quality of USDA gridded crop condition layers *Agrosyst. Geosci. & Environ.* **8** e70087

Bundy L R, Gensini V A, Ashley W S, Haberlie A M and Changnon D 2024 United States crop conditions: 1986–2022 *Agron. J.* **116** 1397–416

Bundy L R, Gensini V A, Ashley W S, Haberlie A M and Changnon D 2026b Surveys and satellites: evaluating crop condition monitoring strategies using field observations and vegetation health indices *Crop Sci.* **66** e70323

Bundy L R, Gensini V A and Van Den Broeke M S 2023 Tropical cyclone impacts on crop condition ratings and yield in the Coastal Southern United States *Agric. For. Meteorol.* **340** 109599

Bundy L R, Kaminski K N, Haberlie A M, Ashley W S and Gensini V A 2026a Derecho impacts on United States crop condition ratings and yield *Agric. For. Meteorol.* **376** 110913

Burchfield E, Matthews-pennanen N, Schoof J and Lant C 2020 Changing yields in the Central United States under climate and technological change *Clim. Change* **159** 329–46

Cai X, Zhang X, Noël P H and Shafiee-jood M 2015 Impacts of climate change on agricultural water management: a review *Wiley Interdiscip. Rev. Water* **2** 439–55

Cannon A J, Sobie S R and Murdock T Q 2015 Bias correction of GCM precipitation by quantile mapping: how well do methods preserve changes in quantiles and extremes? *J. Clim.* **28** 6938–59

Chai Q, Gan Y, Zhao C, Xu H L, Waskom R M, Niu Y and Siddique K H 2016 Regulated deficit irrigation for crop production under drought stress. A review *Agron. Sustain. Dev.* **36** 3

Changnon D and Gensini V A 2019 Changing spatiotemporal patterns of 5- and 10-day Illinois heavy precipitation amounts, 1900–2018 *J. Appl. Meteorol. Climatol.* **58** 1523–33

Chen L and Ford T W 2023 Future changes in the transitions of monthly-to-seasonal precipitation extremes over the Midwest in coupled model Intercomparison Project Phase 6 models *Int. J. Climatol.* **43** 255–74

Chen T and Guestrin C 2016 XGBoost: a scalable tree boosting system. In *Proc. 22nd ACM SIGKDD Int. Conf. on Knowledge Discovery and Data Mining* (Association for Computing Machinery) (https://doi.org/10.1145/2939672.2939785)

Cooter E J, Bash J O, Benson V and Ran L 2012 Linking agricultural crop management and air quality models for regional to national-scale nitrogen assessments *Biogeosciences* **9** 4023–35

Creighton G, Kuchera E, Adams-selin R, McCormick J, Rentschler S and Wickard B 2014 AFWA diagnostics in WRF *Weather Group Document* 2nd edn (Air Force Weather Agency) p 17 (available at: www2.mmm.ucar.edu/wrf/users/docs/AFWA_Diagnostics_in_WRF.pdf)

Daly C, Neilson R P and Phillips D L 1994 A statistical-topographic model for mapping climatological precipitation over mountainous terrain *J. Appl. Meteorol.* **33** 140–58

Deines J M, Kendall A D, Butler J J and Hyndman D W 2019 Quantifying irrigation adaptation strategies in response to stakeholder-driven groundwater management in the US High Plains Aquifer *Environ. Res. Lett.* **14** 044014

Delgado J A, Nearing M A and Rice C W 2013 Conservation practices for climate change adaptation *Advances in Agronomy* ed D L Sparks (Academic) vol 121 pp 47–115

Dittus A J, Karoly D J, Lewis S C and Alexander L V 2015 A multiregion assessment of observed changes in the areal extent of temperature and precipitation extremes *J. Clim.* **28** 9206–20

Easterling D R, Kunkel K E, Arnold J R, Knutson T, LeGrande A N, Leung L R, Vose R S, Waliser D E and Wehner M F 2017 Precipitation change in the United States *Climate Science Special Report: Fourth National Climate Assessment, Volume I* ed D J Wuebbles, D W Fahey, K A Hibbard, D J Dokken, B C Stewart and T K Maycock (U.S. Global Change Research Program) pp 207–30

Fei C, Jägermeyr J, McCarl B, Contreras E M, Mutter C, Phillips M and Vargo A 2023 Future climate change impacts on US agricultural yields, production, and market *Anthropocene* **42** 100386

Fernandez-Perez A, Frijns B, Indriawan I and Tourani-rad A 2019 Surprise and dispersion: informational impact of USDA announcements *Agric. Econ.* **50** 113–26

Food and Agriculture Organization of the United Nations (FAO) 2018 *The State of Agricultural Commodity Markets 2018: Agricultural Trade, Climate Change and Food Security* (FAO) (available at: www.fao.org/3/I9542EN/i9542en.pdf)

Gensini V A 2021 Severe convective storms in a changing climate *Climate Change and Extreme Events* ed A Fares (Springer) pp xx

Gensini V A, Ashley W S, Michaelis A C, Haberlie A M, Goodin J and Wallace B C 2024 Hailstone size dichotomy in a warming climate *npj Clim. Atmos. Sci.* **7** 185

Gensini V A and Brooks H E 2018 Spatial trends in United States tornado frequency *npj Clim. Atmos. Sci.* **1** 38

Gensini V A, Haberlie A M and Ashley W S 2023 Convection-permitting simulations of historical and possible future climate over the contiguous United States *Clim. Dyn.* **60** 109–26

Gerik T, Bean B and Vanderlip R 2024 Sorghum growth and development (available at: https://oaktrust.library.tamu.edu/server/api/core/bitstreams/0d55712d-0172-48d4-b597-b8a4765b9ed2/content)

Glauber J 2023 *Rethinking Trade Rules to Achieve a More Climate Resilient Agriculture* vol 2164 (Intl Food Policy Res Inst)

Haberlie A M, Wallace B, Ashley W S, Gensini V A and Michaelis A C 2024 Mesoscale convective system activity in the United States under intermediate and extreme climate change scenarios *Clim. Change* **177** 94

Hargreaves G H 1994 Defining and using reference evapotranspiration *J. Irrig. Drain. Eng.* **120** 1132–9

Hargreaves G H and Allen R G 2003 History and evaluation of Hargreaves evapotranspiration equation *J. Irrig. Drain. Eng.* **129** 53–63

Hargreaves G H and Samani Z A 1982 Estimating potential evapotranspiration *J. Irrig. Drain. Div.* **108** 225–30

Hatfield J L, Boote K J, Kimball B A, Ziska L H, Izaurralde R C, Ort D, Thomson A M and Wolfe D 2011 Climate impacts on agriculture: implications for crop production *Agron. J.* **103** 351–70

Hatfield J L and Dold C 2019 Water-use efficiency: advances and challenges in a changing climate *Front. Plant Sci.* **10** 103

Hatfield J L and Prueger J H 2015 Temperature extremes: effect on plant growth and development *Weather Clim. Extrem.* **10** 4–10

Hatfield J, Swanston C, Janowiak M, Steele R F, Hempel J, Bochicchio J, Hall W, Cole M, Hestvik S and Whitaker J 2015 *USDA Midwest and Northern Forests Regional Climate Hub: Assessment of Climate Change Vulnerability and Adaptation and Mitigation Strategies* (U.S. Department of Agriculture) pp 55 (available at: www.climatehubs.usda.gov/sites/default/files/Midwest%20Region%20Vulnerability%20Assessment%203_20_2015.pdf)

Hausfather Z and Peters G P 2020 Emissions–the 'business as usual' story is misleading *Nature* **577** 618–20

Huffman W E, Jin Y and Xu Z 2018 The economic impacts of technology and climate change: new evidence from US corn yields *Agric. Econ.* **49** 463–79

Hultgren A, Carleton T, Delgado M, Gergel D R, Greenstone M, Houser T and Yuan J 2025 Impacts of climate change on global agriculture accounting for adaptation *Nature* **642** 644–52

Huntington T, Cui X, Mishra U and Scown C D 2020 Machine learning to predict biomass sorghum yields under future climate scenarios *Biofuels Bioprod. Biorefin.* **14** 566–77

Hurburgh C 2016 *Wet Weather Creates challenges for Harvest* (Iowa State University Extension and Outreach) (available at: https://crops.extension.iastate.edu/cropnews/2016/09/wet-weather-creates-challenges-harvest)

Hurrell J W *et al* 2013 The community earth system model: a framework for collaborative research *Bull. Am. Meteorol. Soc.* **94** 1339–60

Intergovernmental Panel on Climate Change (IPCC) 2022 *Climate Change 2022: Impacts, Adaptation, and Vulnerability (Working Group II Contribution to the Sixth Assessment Report)* (Cambridge University Press) (https://doi.org/10.1017/9781009325844)

Intergovernmental Panel on Climate Change 2014 Climate change 2014: synthesis report (IPCC) p 151 (available at: www.ipcc.ch/report/ar5/syr/)

Irwin S and Good D 2017a When should we start paying attention to crop condition ratings for corn and soybeans? *Farmdoc Daily* **7** (available at: https://farmdocdaily.illinois.edu/2017/05/when-start-paying-attention-crop-condition-ratings.html)

Irwin S and Good D 2017b How should we use within-season crop condition ratings for corn and soybeans? *Farmdoc Daily* **7** (available at: https://farmdocdaily.illinois.edu/2017/06/how-to-use-within-season-crop-condition-ratings.html)

Irwin S and Hubbs T 2018a Measuring the accuracy of forecasting corn and soybean yield with good and excellent crop condition ratings *Farmdoc Daily* **8** (available at: https://farmdocdaily.illinois.edu/2018/06/measuring-the-accuracy-of-forecasting-corn-and-soybean-yield.html)

Irwin S and Hubbs T 2018b Does the bias in early season crop condition ratings for corn and soybeans vary with the magnitude of the ratings? *Farmdoc Daily* **8** (available at: https://farmdocdaily.illinois.edu/2018/06/bias-in-early-season-crop-condition-ratings.html)

Jägermeyr J, Müller C, Ruane A C, Elliott J, Balkovic J, Castillo O and Rosenzweig C 2021 Climate impacts on global agriculture emerge earlier in new generation of climate and crop models *Nat. Food* **2** 873–85

Jin Z, Zhuang Q, Wang J, Archontoulis S V, Zobel Z and Kotamarthi V R 2017 The combined and separate impacts of climate extremes on the current and future U.S. rainfed maize and soybean production under elevated CO_2 *Glob. Change Biol.* **23** 2687–704

Jinger D, Kaur R, Kaur N, Rajanna G A, Kumari K and Dass A 2017 Weed dynamics under changing climate scenario: a review *Int. J. Curr. Microbiol. Appl. Sci.* **6** 2376–88

Jung J, Maeda M, Chang A, Bhandari M, Ashapure A and Landivar-bowles J 2021 The potential of remote sensing and artificial intelligence as tools to improve the resilience of agriculture production systems *Curr. Opin. Biotechnol.* **70** 15–22

Kaminski K, Ashley W S, Haberlie A M and Gensini V A 2025 Future derecho potential in the United States *J. Clim.* **38** 3–26

Karali B, Isengildina-massa O, Irwin S H and Adjemian M K 2016 *Changes in informational value and the market reaction to USDA reports in the big data era* (AgEcon Search) (available at: https://ageconsearch.umn.edu/record/235580/)

Kaur G, Zurweller B A, Nelson K A, Motavalli P P and Dudenhoeffer C J 2017 Soil waterlogging and nitrogen fertilizer management effects on corn and soybean yields *Agron. J.* **109** 97–106

Kendon E J, Ban N, Roberts N M, Fowler H J, Roberts M J, Chan S C and Wilkinson J M 2017 Do convection-permitting regional climate models improve projections of future precipitation change? *Bull. Am. Meteorol. Soc.* **98** 79–93

Khaki S, Pham H and Wang L 2021 Simultaneous corn and soybean yield prediction from remote sensing data using deep transfer learning *Sci. Rep.* **11** 1–14

Kukal M S and Irmak S 2018 Climate-driven crop yield and yield variability and climate change impacts on the US Great Plains agricultural production *Sci. Rep.* **8** 1–18

Lasher-Trapp S, Orendorf S A and Trapp R J 2023 Investigating a derecho in a future warmer climate *Bull. Am. Meteorol. Soc.* **104** E1831–E52

Lauer J 2012 The effects of drought and poor corn pollination on corn *Field Crops* **28** 493–5 (available at: https://corn.agronomy.wisc.edu/AA/pdfs/A095.pdf)

Lehecka G V 2014 The value of USDA crop progress and condition information: reactions of corn and soybean futures markets *J. Agric. Resour. Econ.* **39** 88–105 (available at: https://www.jstor.org/stable/44131316)

Li Y, Guan K, Schnitkey G D, DeLucia E and Peng B 2019 Excessive rainfall leads to maize yield loss of a comparable magnitude to extreme drought in the United States *Glob. Change Biol.* **25** 2325–37

Lin T S, Song Y, Lawrence P, Kheshgi H S and Jain A K 2021 Worldwide maize and soybean yield response to environmental and management factors over the 20th and 21st centuries *J. Geophys. Res. Biogeosci.* **126** e2021JG006304

Lobell D B and Asseng S 2017 Comparing estimates of climate change impacts from process-based and statistical crop models *Environ. Res. Lett.* **12** 015001

Lobell D B and Gourdji S M 2012 The influence of climate change on global crop productivity *Plant Physiol.* **160** 1686–97

Lobell D B, Roberts M J, Schlenker W, Braun N, Little B B, Rejesus R M and Hammer G L 2014 Greater sensitivity to drought accompanies maize yield increase in the U.S. Midwest *Science* **344** 516–9

Manabe S 1969 Climate and the ocean circulation: i. The atmospheric circulation and the hydrology of the earth's surface *Mon. Weather Rev.* **97** 739–74

Mariadass D A, Moung E G, Sufian M M and Farzamnia A 2022 Extreme gradient boosting (XGBoost) regressor and Shapley additive explanations for crop yield prediction in agriculture *2022 12th Int. Conf. on Computer and Knowledge Engineering (ICCKE)* (IEEE) pp 219–24

Martin J T, Pederson G T, Woodhouse C A, Cook E R, McCabe G J, Anchukaitis K J and King J 2020 Increased drought severity tracks warming in the United States' largest river basin *Proc. Natl Acad. Sci. USA* **117** 11328–36

McGuire V L 2017 *Water-level and Recoverable Water in Storage Changes, High Plains Aquifer, Predevelopment to 2015 and 2013–15* No. 2017–5040 (US Geological Survey) (https://doi.org/10.3133/sir20175040)

McKenzie A M and Ke Y 2022 How do USDA announcements affect international commodity prices? *J. Commodity Mark.* **28** 100239

Moss R H *et al* 2010 The next generation of scenarios for climate change research and assessment *Nature* **463** 747–56

Mourtzinis S, Specht J E, Lindsey L E, Wiebold W J, Ross J, Nafziger E D and Conley S P 2015 Climate-induced reduction in US-wide soybean yields underpinned by region-and in-season-specific responses *Nat. Plants* **1** 1–4

Na W and Najafi M R 2024 Rising risks of hydroclimatic swings: a large ensemble study of dry and wet spell transitions in North America *Glob. Planet. Change* **238** 104476

Petersen L K 2019 Impact of climate change on twenty-first century crop yields in the US *Climate* **7** 40

Porter J R and Gawith M 1999 Temperatures and the growth and development of wheat: a review *Eur. J. Agron.* **10** 23–36

Prein A F *et al* 2015 A review on regional convection-permitting climate modeling: demonstrations, prospects, and challenges *Rev. Geophys.* **53** 323–61

PRISM Climate Group 2025 *PRISM Climate Group* (Northwest Alliance for Computational Science and Engineering) (available at: www.prism.oregonstate.edu/)

Proctor J, Zeppetello L V, Chan D and Huybers P 2025 Climate change increases the interannual variance of summer crop yields globally through changes in temperature and water supply *Sci. Adv.* **11** eady3575

Ramesh K, Matloob A, Aslam F, Florentine S K and Chauhan B S 2017 Weeds in a changing climate: vulnerabilities, consequences, and implications for future weed management *Front. Plant Sci.* **8** 95

Rezaei E E, Webber H, Asseng S, Boote K, Durand J L, Ewert F and MacCarthy D S 2023 Climate change impacts on crop yields *Nat. Rev. Earth Environ.* **4** 831–46

Roberts M J, Braun N O, Sinclair T R, Lobell D B and Schlenker W 2017 Comparing and combining process-based crop models and statistical models with some implications for climate change *Environ. Res. Lett.* **12** 095010

Rosales A 2021 *Crop progress and condition layers* (U.S. Department of Agriculture, National Agricultural Statistics Service) (available at: www.nass.usda.gov/Research_and_Science/Crop_Progress_Gridded_Layers/CropProgressDescription.pdf)

Rosenzweig C, Elliott J, Deryng D, Ruane A C, Müller C, Arneth A and Jones J W 2014 Assessing agricultural risks of climate change in the twenty-first century in a global gridded crop model intercomparison *Proc. Natl Acad. Sci. USA* **111** 3268–73

Sacks W J and Kucharik C J 2011 Crop management and phenology trends in the US Corn Belt: impacts on yields, evapotranspiration and energy balance *Agric. For. Meteorol.* **151** 882–94

Scanlon B R, Faunt C C, Longuevergne L, Reedy R C, Alley W M, McGuire V L and McMahon P B 2012 Groundwater depletion and sustainability of irrigation in the US high plains and central valley *Proc. Natl Acad. Sci. USA* **109** 9320–5

Schauberger B, Archontoulis S, Arneth A, Balkovic J, Ciais P, Deryng D and Frieler K 2017 Consistent negative response of US crops to high temperatures in observations and crop models *Nat. Commun.* **8** 13931

Schlenker W and Roberts M J 2009 Nonlinear temperature effects indicate severe damages to US crop yields under climate change *Proc. Natl Acad. Sci. USA* **106** 15594–8

Schulte L A, Niemi J, Helmers M J, Liebman M, Arbuckle J G, James D E and Witte C 2017 Prairie strips improve biodiversity and the delivery of multiple ecosystem services from corn–soybean croplands *Proc. Natl Acad. Sci. USA* **114** 11247–52

Schwalm C R, Glendon S and Duffy P B 2020 RCP8. 5 tracks cumulative CO_2 emissions *Proc. Natl Acad. Sci. USA* **117** 19656–7

Skamarock W C *et al* 2019 *A Description of the Advanced Research WRF Model Version 4* NCAR Technical Note NCAR/TN-556+STR (National Center for Atmospheric Research) p 145

Skamarock W C and Klemp J B 2008 A time-split nonhydrostatic atmospheric model for weather research and forecasting applications *J. Comput. Phys.* **227** 3465–85

Slafer G A and Rawson H M 1994 Sensitivity of wheat phasic development to major environmental factors: a re-examination of some assumptions made by physiologists and modellers *Funct. Plant Biol.* **21** 393–426

Stinnett S N, Gensini V A, Haberlie A M, Michaelis A C and Ashley W S 2024 Changes in extreme daily precipitation over the contiguous United States from convection-permitting simulations *J. Appl. Meteorol. Climatol.* **63** 1523–43

Sutton E, Jain M, Connell K, Wang H, Zhou W, Deshpande M and Blesh J 2025 Increasing crop rotation diversity with cover crops builds climate resilience on farms *Environ. Res. Lett.* **20** 124025

Tack J, Barkley A and Nalley L L 2015 Effect of warming temperatures on US wheat yields *Proc. Natl Acad. Sci. USA* **112** 6931–6

Tang B H, Gensini V A and Homeyer C R 2019 Trends in United States large hail environments and observations *npj Clim. Atmos. Sci.* **2** 45

Taylor K E, Stouffer R J and Meehl G A 2012 An overview of CMIP5 and the experiment design *Bull. Am. Meteorol. Soc.* **93** 485–98

Tebaldi C, Debeire K, Eyring V, Fischer E, Fyfe J, Friedlingstein P and Ziehn T 2021 Climate model projections from the scenario model intercomparison project (ScenarioMIP) of CMIP6 *Earth Syst. Dyn.* **12** 253–93

Thornthwaite C W 1948 An approach toward a rational classification of climate *Geogr. Rev.* **38** 55–94

Thornthwaite C W and Mather J R 1955 The water balance *Publ. Climatol.* **8** 1–104

Thornthwaite C W and Mather J R 1957 Instructions and tables for computing potential evapotranspiration and the water balance *Publications in Climatology* vol 10 (Laboratory of Climatology, Drexel Institute of Technology)

U.S. Department of Agriculture, National Agricultural Statistics Service 2016 *Crop progress/crop weather terms and definitions* (available at: www.nass.usda.gov/Publications/National_Crop_Progress/terms_definitions)

U.S. Department of Agriculture, National Agricultural Statistics Service 2025a *Quick stats* (available at: https://quickstats.nass.usda.gov/)

U.S. Department of Agriculture 2025b *Crop Progress* (Cornell University Library (USDA Economics, Statistics and Market Information System)) (available at: https://usda.library.cornell.edu/concern/publications/8336h188j)

Vose R S, Easterling D R, Kunkel K E, LeGrande A N and Wehner M F 2017 Temperature changes in the United States *Climate Science Special Report: Fourth National Climate Assessment, Volume I* ed D J Wuebbles, D W Fahey, K A Hibbard, D J Dokken, B C Stewart and T K Maycock (U.S. Global Change Research Program) pp 185–206

Waldhoff S T, Wing I S, Edmonds J, Leng G and Zhang X 2020 Future climate impacts on global agricultural yields over the 21st century *Environ. Res. Lett.* **15** 114010

Wallace B, Haberlie A M, Gensini V A, Ashley W S and Michaelis A C 2025 Cause and characteristics of changes in mesoscale convective systems within a convection-permitting regional climate model *J. Clim.* **38** 461–79

Walthall C L *et al* 2012 Climate change and agriculture in the United States: effects and adaptation USDA Technical Bulletin No. 1935 (U.S. Department of Agriculture) (available at: www.usda.gov/sites/default/files/documents/CC_and_Ag_US_1935.pdf)

Wehner M F, Arnold J R, Knutson T, Kunkel K E and LeGrande A N 2017 Droughts, floods, and wildfires *Climate Science Special Report: Fourth National Climate Assessment, Volume I* ed D J Wuebbles, D W Fahey, K A Hibbard, D J Dokken, B C Stewart and T K Maycock (U.S. Global Change Research Program) pp 231–56

Weisman M L, Skamarock W C and Klemp J B 1997 The resolution dependence of explicitly modeled convective systems *Mon. Weather Rev.* **125** 527–48

Welch B L 1947 The generalization of "Student's" problem when several different population variances are involved *Biometrika* **34** 28–35

Westcott P C and Jewison M 2013 Weather effects on expected corn and soybean yields (available at: www.ers.usda.gov/publications/pub-details?pubid=36652)

Westenbroek S M, Engott J A, Kelson V A and Hunt R J 2018 *SWB Version 2.0—A Soil-water-balance Code for Estimating Net Infiltration and Other Water-budget Components* (*Techniques and Methods, Book 6, Chap. A59*) (U.S. Geological Survey) (https://doi.org/10.3133/tm6A59)

Westra S *et al* 2014 Future changes to the intensity and frequency of short-duration extreme rainfall *Rev. Geophys.* **52** 522–55

Wienhold B J, Vigil M F, Hendrickson J R and Derner J D 2018 Vulnerability of crops and croplands in the US Northern Plains to predicted climate change *Clim. Change* **146** 219–30

Wilson A B *et al* 2023 Midwest *Fifth National Climate Assessment* ed A R Crimmins, C W Avery, D R Easterling, K E Kunkel, B C Stewart and T K Maycock (U.S. Global Change Research Program) ch 24 (https://doi.org/10.7930/NCA5.2023.CH24)

Zeeb A W, Ashley W S, Haberlie A M, Gensini V A and Michaelis A C 2024 Supercell precipitation contribution to the United States hydroclimate *Int. J. Climatol.* **44** 1489–512

Zhu X, Troy T J and Devineni N 2019 Stochastically modeling the projected impacts of climate change on rainfed and irrigated US crop yields *Environ. Res. Lett.* **14** 074021

Zonta J H, Brandao Z N, Rodrigues J I D S and Sofiatti V 2017 Cotton response to water deficits at different growth stages *Rev. Caatinga* **30** 980–90